Best Available

Copy

for all Pictures

AD-787 497

OPTICALLY PUMPED LASER

Robert T. Brown

United Aircraft Research Laboratories

Prepared for:

Office of Naval Research
Advanced Projects Agency

10 October 1974

DISTRIBUTED BY:

NTIS
National Technical Information Service
U. S. DEPARTMENT OF COMMERCE

SECURITY CLASSIFICATION OF THIS PAGE (When Data Entered)

REPORT DOCUMENTATION PAGE

READ INSTRUCTIONS BEFORE COMPLETING FORM

1. REPORT NUMBER: N921853-2

2. GOVT ACCESSION NO.:

3. RECIPIENT'S CATALOG NUMBER:

4. TITLE (and Subtitle): OPTICALLY PUMPED LASER

5. TYPE OF REPORT & PERIOD COVERED: 3/1/74 - 8/15/74 Semi-Annual Tech.

6. PERFORMING ORG. REPORT NUMBER: N921853-2

7. AUTHOR(s): Robert T. Brown

8. CONTRACT OR GRANT NUMBER(s): N00014-74-C-0376

9. PERFORMING ORGANIZATION NAME AND ADDRESS:
United Aircraft Research Laboratories
400 Main Street
East Hartford, Conn. 06108

10. PROGRAM ELEMENT, PROJECT, TASK AREA & WORK UNIT NUMBERS: ARPA

11. CONTROLLING OFFICE NAME AND ADDRESS:
Office of Naval Research
Department of Navy
Arlington, VA 22217

12. REPORT DATE: 10/15/74

13. NUMBER OF PAGES: 60

14. MONITORING AGENCY NAME & ADDRESS (if different from Controlling Office):
Director, Physics Programs
Physical Sciences Division
Office of Naval Research
800 N. Quincy Street, Arlington, VA 22217

15. SECURITY CLASS. (of this report): Unclassified

15a. DECLASSIFICATION/DOWNGRADING SCHEDULE:

16. DISTRIBUTION STATEMENT (of this Report):

DISTRIBUTION STATEMENT A
Approved for public release;
Distribution Unlimited

17. DISTRIBUTION STATEMENT (of the abstract entered in Block 20, if different from Report):

18. SUPPLEMENTARY NOTES:

19. KEY WORDS (Continue on reverse side if necessary and identify by block number):

Optically-pumped electric-discharge laser
uv laser
Excimer

Reproduced by
NATIONAL TECHNICAL INFORMATION SERVICE
U S Department of Commerce
Springfield VA 22151

20. ABSTRACT (Continue on reverse side if necessary and identify by block number):

This report describes experimental and theoretical studies of a new technique for pumping high-pressure electric-discharge lasers. Diffuse discharges in mixtures of He/N_2 and $He/N_2/Ar$ at electron densities in excess of $10^{15} cm^{-3}$ and pressures of 15 atm were obtained. Calculations for a He/Xe mixture operating on the 1730Å transition in molecular Xe show efficiencies for conversion from the 10.6μ field into the uv radiation field in escess of 60%. Kinetic studies of the excimer energy transfer in $He/Ar/N_2$ mixtures are described along with new pumping

DD FORM 1 JAN 73 1473 EDITION OF 1 NOV 65 IS OBSOLETE

SECURITY CLASSIFICATION OF THIS PAGE (When Data Entered)

Block 20

configurations which will allow operation with a uv optical cavity.

UNITED AIRCRAFT CORPORATION
RESEARCH LABORATORIES

Report Number: N-921853-2
Semi-Annual Technical Report for the period
1 March 1974 to 15 August 1974

OPTICALLY PUMPED LASER

ARPA Order No.:	1807
Program Code:	4E90K21
Contractor:	United Aircraft Research Laboratories
Effective Date of Contract:	1 March 1974
Contract Expiration Date:	15 October 1974
Amount of Contract:	$55,205
Contract Number:	N00014-74-C-0376
Principal Investigator:	Dr. David C. Smith (203) 565-5281
Scientific Officer:	Director, Physics Programs Physical Sciences Division Office of Naval Research Department of the Navy 800 North Quincy Street Arlington, VA 22217
Short Title:	Optically Pumped Lasers
Report by:	R. T. Brown

The views and conclusions contained in this document are those of the author and should not be interpreted as necessarily representing the official policies, either expressed or implied, of the Advanced Research Projects Agency or the U. S. Government.

Sponsored By
Advanced Research Projects Agency
ARPA Order No. 1807

UNITED AIRCRAFT RESEARCH LABORATORIES

SEMI-ANNUAL REPORT N921853-2

TABLE OF CONTENTS

	Page
TECHNICAL REPORT SUMMARY	1
I. INTRODUCTION	4
II. KINETIC PROCESSES IN OPTICALLY PUMPED ELECTRIC DISCHARGE EXCIMER LASERS	6
2.1 BACKGROUND	6
2.2 CASE 1 - LARGE SYSTEM, NO OPTICAL CAVITY, QUASI-STEADY STATE	9
2.3 CASE 2 - LARGE SYSTEM, OPTICAL CAVITY, QUASI-STEADY STATE	9
2.4 SCALING AND EFFICIENCY CONSIDERATIONS	10
III. NUMERICAL MODELING STUDIES	12
3.1 DESCRIPTION OF THE MODEL	12
3.2 TYPICAL RESULTS	18
IV. EXPERIMENTAL FACILITY	22
4.1 TEA LASER	22
4.2 GAS HANDLING SYSTEM	26
4.3 TEST CELLS	26
4.4 DIAGNOSTICS	26
V. EXPERIMENTAL RESULTS	29
5.1 INTRODUCTION	29
5.2 COAXIAL DISCHARGE STUDIES AT HIGH PRESSURE	29
5.3 TRANSVERSE PUMPING STUDIES	32

TABLE OF CONTENTS (Con't)

	Page
5.4 KINETIC STUDIES	36
5.5 LASER STUDIES	40
VI. PUMPING CONFIGURATION STUDIES	43
6.1 INTRODUCTION	43
6.2 DESCRIPTION	43
6.3 EXPERIMENTAL STUDIES	43
VII, SUMMARY & CONCLUSIONS	50
REFERENCES	51
APPENCIX	52

FIGURE CAPTIONS

Figure		Page
I-1.	Experimental arrangement used in preliminary experiments.	5
II-1.	Approximate xenon kinetic model.	7
III-1.	Schematic energy level diagram for xenon.	13
III-2.	Calculated results for OPEDL in He/Xe - small system. $p_{Xe} = 4.8$ atm, $p_{He} = 11.2$ atm, $w = h = 0.1$ cm, $L_d = 4.0$ cm, $R_1 = 0.80$, $R_2 = 0.88$.	14
III-3.	Calculated results for OPEDL in Xe-large system. $p_{Xe} = 16.0$ atm, $p_{He} = 0$, $w = h = 1.0$ cm, $L_d = 100$ cm, $R_1 = 0.20$, $R_2 = 0.88$.	19
III-4.	Calculated results for OPEDL in Xe-quasi-steady solution. $p_{Xe} = 16.0$ atm, $p_{He} = 0$, $w = h = 1.0$ cm, $L_d = 100$ cm, $R_1 = 0.20$, $R_2 = 0.88$.	20
III-5.	Calculated results for OPEDL in Xe - high initial electron density. $p_{Xe} = 16.0$ atm, $p_{He} = 0$, $w = h = 1.0$ cm, $L_d = 100$ cm, $R_1 = 0.20$, $R_2 = 0.88$.	21
IV-1.	Diagram of TEA laser system.	23
IV-2.	Photograph of experiment.	24
IV-3.	Near-field laser burn pattern and TEA laser pulse shape.	25
IV-4.	Transverse pumping configuration.	27
IV-5.	Photograph of transverse pumping cell.	28
V-1.	Optically-pumped discharges in He/N_2. (a) Test cell. (b) Diffuse discharge. (c) Aerosol-induced breakdowns.	30
V-2	Optically-pumped discharges in He/N_2. (a) $p = 7.1$ atm. $X_{N_2} = 0.14$, (b) $p = 7.1$ atm, $X_{N_2} = 0.12$, (c) $p = 12.0$ atm, $I_o = 6.0 \times 10^8$ W/cm^2. (d) $p = 12.0$ atm, $I_o = 7.0 \times 10^8$ W/cm^2.	31

		Page
V-3.	Optically-pumped discharges in He/Ar/N_2. (a) p = 10.0 atm, I_o = 4.2 x 10^8 W/cm^2. (b) p = 15.0 atm, I_o = 6.0 x 10^8 W/cm^2.	33
V-4.	Optically-pumped discharges in He/Ar.	34
V-5.	Transverse pumping photos.	35
V-6.	3371Å Spontaneous emission signals at high nitrogen partial pressures.	37
V-7.	3371Å Spontaneous emission signals at low nitrogen partial pressure.	38
V-8.	3371Å Spontaneous emission signals in He/Ar/N_2 mixtures.	39
V-9.	uv Cavity arrangement.	41
V-10	Photodetector traces with uv cavity.	42
VI-1.	Annular-cone pumping configuration.	44
VI-2.	Beam profiles at various locations.	45
VI-3.	Gas breakdown in lab air with annular-cone beam.	46
VI-4.	Axial intensity distribution with annular-cone beam.	48
VI-5.	Transverse intensity distribution with annular-cone beam.	49

TECHNICAL REPORT SUMMARY

Under this contract, a new technique for pumping high-pressure electric-discharge laser media is being investigated. The objective of this program is to develop high-energy, high-efficiency lasers operating in the ultraviolet and visible portions of the spectrum.

This report covers the Fiscal 1974 interim program. The objectives of this program were to develop hardware, to perform calculations, and to make preliminary measurements in preparation for an in-depth, one-year study in Fiscal 1975. The theory described in this report evolved out of a simplified kinetic model for xenon, developed under a Corporate-sponsored program, and the experiments evolved out of studies carried out in a one-atmosphere mixture of He/N_2. The present program is primarily experimental in nature, and a large portion of the FY'74 effort went into designing and fabricating the test cells, gas handling system, and diagnostic systems, and into upgrading the TEA laser facility. A number of very excouraging experimental results were obtained however, with intense diffuse discharges being generated in Ar/N_2 and $He/Ar/N_2$ mixtures at pressures up to 15 atm.

As anticipated, experimental studies showed that diffuse discharges in noble gases at high pressure are more difficult to obtain than in He/N_2 mixtures at atmospheric pressure. This was due to the increased sensitivity of the discharge to non-uniformities in the intensity of the pumping radiation and increased sensitivity to aerosols present in the cell, with both effects leading to gas breakdown rather than a diffuse discharge. It was found that the addition of helium as a buffer gas reduced the tendency to form gas breakdown spots in the optically-pumped discharge. By the end of the FY'74 program, considerable improvement had been made in the beam quality and pulse-to-pulse repeatability of the TEA laser and in eliminating aerosols from the cell, allowing the attainment of diffuse discharges at several atmospheres of helium/argon.

While the helium/argon mixtures were prone to gas breakdown, it was fairly easy to obtain diffuse discharges in mixtures of He/N_2 and $He/Ar/N_2$ and diffuse discharges were obtained in such mixtures at pressures up to 15 atm. For this reason, most of the experimental data taken during this report period deal with $He/Ar/N_2$ rather than He/Xe.

While the $He/Ar/N_2$ system appears to be easier to work with experimentally, the kinetics are more complicated and the various rates are not as well known as for xenon. Most of the theoretical results obtained during this report period are for xenon and Xe/He mixtures. Theoretical studies of $He/Ar/N_2$

are currently in progress.

Section II is an approximate analysis of the xenon excimer laser (1730Å) and is valid for pressures above ~10 atm. This analysis gives a simple, but accurate, explanation of the attractive efficiency and scalability of the optically-pumped electric discharge laser (OPEDL) concept applied to high-pressure excimer systems.

Section III describes a more sophisticated numerical model which is valid for mixtures of He/Xe and pressures in the 1-20 atm range. This code is being used to model conditions which it is anticipated can readily be produced in the experiments (i.e., pressures in the 3-10 atm range.)

Section IV is a description of the experimental facility. During this report period the entire experiment was moved to a larger laboratory and the various elements in the optical train were mounted on a stable optical table. Various improvements in the system were made to improve the long term stability, repeatability, and useability of the experiment. Test cells and a gas handling system were developed which are capable of being pumped to 10^{-6} torr and back-filled with filtered gas at pressures up to 20 atm. A shielded diagnostic system was assembled which has the sensitivity and time response necessary for measuring the radiation of interest for the various transitions from 1700 Å to 5000 Å.

Section V is a discussion of the experimental results. Diffuse discharges in mixtures of He/N_2 and $He/N_2/Ar$ at electron densities in excess of $10^{15}cm^{-3}$ and pressures of 15 atm were obtained. These results are significant, since they represent the first time that high-electron density, high-pressure discharges have been obtained by a technique other than use of a high-energy electron beam. Measurements of the 3371 Å spontaneous emission in $He/Ar/N_2$ show that the discharge couples to the excimer level of Ar, which in turn couples to the $C^3\pi$ state of N_2, with the decay time varying from ~3 nsec at high N_2 concentrations to ~500 nsec at high Ar, low N_2 concentrations. This result indicates that the Ar/N_2 excimer-transfer laser is a promising candidate for the OPEDL technique. Preliminary attempts were made to observe uv lasing in the $He/Ar/N_2$ mixture. These attempts were unsuccessful, due primarily to the lack of an appropriate optical configuration. These cavity studies will be continued in the near future with an improved optical configuration.

As mentioned above, optical cavity studies were hampered by lack of an appropriate pumping configuration. It was initially planned to use a transverse pumping configuration, similar to the E-beam studies, by utilizing a cylindrical mirror. However, non-uniformities in the TEA laser transverse profile caused hot spots at the focus, resulting in pumping at discrete points

rather than over a large volume. This was a disappointing result and indicates that with the present laser, transverse pumping using a cylindrical mirror is probably not feasible. On the other hand, focusing the pumping radiation with a cylindrical mirror gave diffuse, quasi-uniform discharges, but required the use of a long uv cavity with various intracavity elements to separate the 10.6μ and uv radiation. To overcome these problems, a novel optical configurations has been developed and is described in Section VI. Preliminary results with this configuration are very encouraging.

Section VII contains a brief summary as well as anticipated activities under the first portion of the FY'75 program.

SECTION I

INTRODUCTION

The objective of this program is to develop high-power, high-efficiency lasers operating in the uv and visible portions of the spectrum. Previous studies in this area have centered around two techniques for generating such pulses. Low inductance circuits have been used to produce fast-rising high-current discharges at moderate pressure in order to pump transitions such as the 3371Å laser transition in molecular nitrogen.[1] More recently, high-energy short-pulse electron beams have been used to produce high-pressure lasers in xenon at 1730Å[2], argon/nitrogen at 3577Å[3], and helium/nitrogen at 4270Å.[4] The present study involves using a high-energy 10.6 μ pulse from a TEA laser to drive a diffuse discharge in a high pressure gas. The properties of this discharge are such that it can be used as the active medium for a uv or visible laser.

The basic elements of this concept can be explained in terms of the arrangement shown in Fig. 1. The outputlaser pulse from the TEA laser is focused into the active uv laser medium which has been preionized to some low level of electron density (in the present studies, the preionization was produced via photoionization from two rows of small arcs in the uv laser medium). The 10.6 μ optical field then heats the electrons via inverse bremsstrahlung, and the electron density grows in a cascade process.[5] The size of the discharge produced is determined by the size of the 10.6 μ laser focal volume. Since this discharge can have a very fast risetime (~10 nsec) and can reach very high electron densities (full ionization, i.e. gas breakdown, for sufficiently high 10.6 μ laser fluxes), the discharge should be suitable for pumping various uv laser transitions.

In preliminary experiments, the concept described above was applied to the 3371Å transition in molecular nitrogen. A detailed description of the results is given in Appendix I. A diffuse discharge was obtained in an atmospheric pressure mixture of helium/nitrogen, and an intense pulse of 3371Å radiation was observed. Under the present contract, this technique is being extended to more difficult but potentially more efficient and useful gas laser media.

FIG. I-1

EXPERIMENTAL ARRANGEMENT USED IN PRELIMINARY EXPERIMENTS

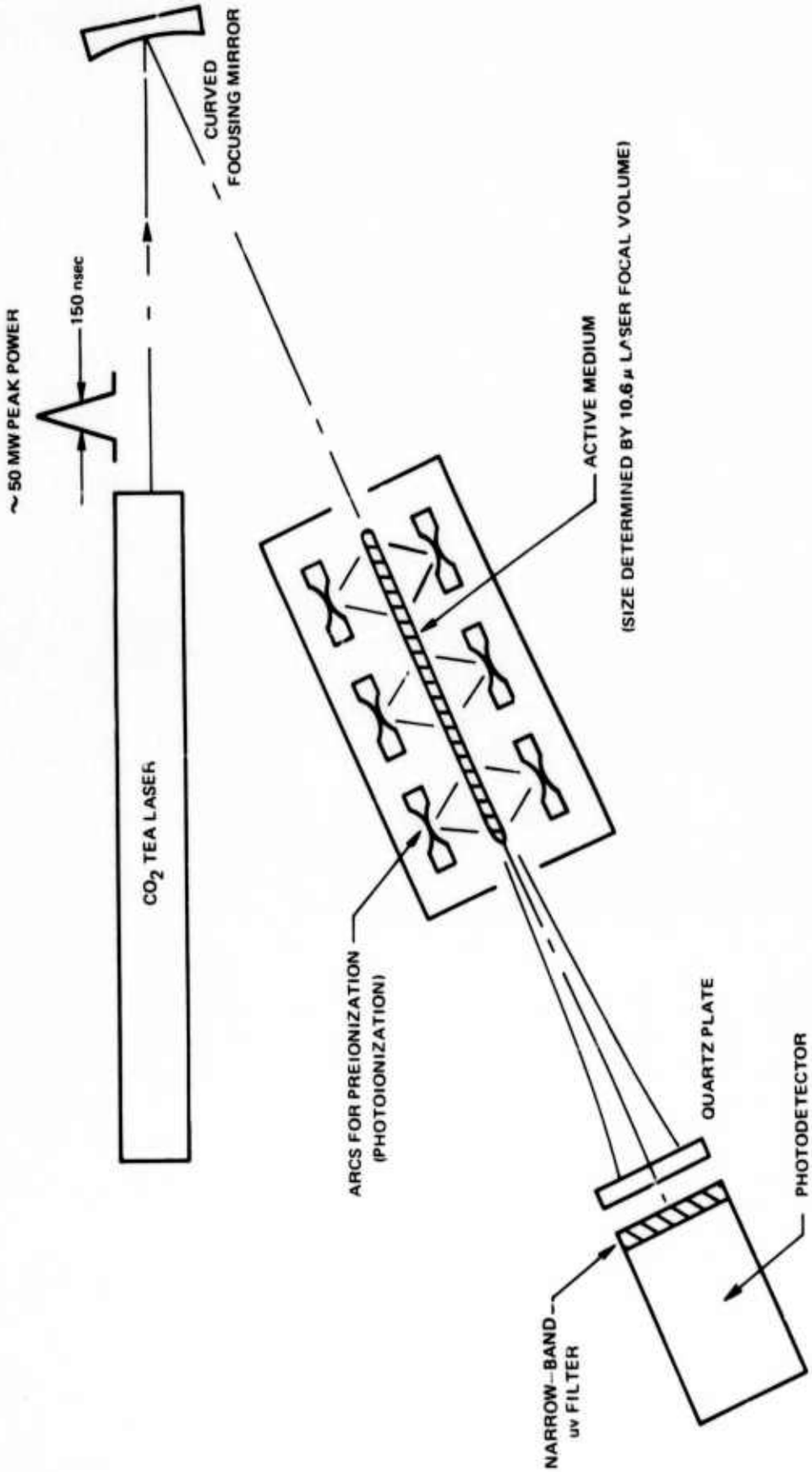

N09-238-11

SECTION II

KINETIC PROCESSES IN OPTICALLY PUMPED ELECTRIC DISCHARGE EXCIMER LASERS

2.1 Background

Kinetic calculations are being carried out for an optically-pumped electric-discharge laser (OPEDL) in mixtures of helium/xenon (1730Å) and for mixtures of helium/argon/nitrogen (3577Å). Since the xenon system is physically simpler than the argon/nitrogen system (fewer important rate processes) and since the various rates for xenon are better known, at present, than for the argon/nitrogen system, the xenon kinetics will be treated in this report, and will be used to illustrate the potentially attractive efficiency and scalability of an OPEDL.

The model used here is similar to that of George[6], with the addition of the inverse bremsstrahlung heating term to the electron energy equation. An approximate form of the kinetic model for pure xenon is illustrated schematically in Fig. II-1. For pressures greater than 10 atm, the rate coefficients in Ref. 7 indicate that atomic ions and excited atoms are converted to molecular ions and excimers on a time scale of ~0.4 nsec. Also, excimers in higher-lying excited states are collisionally deexcited to the lowest excimer level on the same time scale. Therefore, for pressures above ~10 atm, these processes can be treated as instantaneous and the three-level excimer model shown in Fig. II-1 is a good approximation.

For this approximate model the rate equations for the electron density [e] and the excimer density $[Xe_2^*]$ can be written

$$\frac{d[e]}{dt} = [e]\,[Xe^o]\,k_1 + [e]\,[Xe_2^*]\,k_3 + [Xe_2^*]^2\,k_5 - [e]^2\,k_4\,, \qquad (1)$$

and

$$\frac{d[Xe_2^*]}{dt} = [e]\,[Xe^o]\,k_2 + [e]^2\,k_4 - [e]\,[Xe_2^*]\,k_3 - [Xe_2^*]^2\,k_5 - [Xe_2^*]\,k_7 - \frac{\sigma_{STE}\,I_{uv}}{(h\upsilon)_{uv}}\,[Xe_2^*], \qquad (2)$$

APPROXIMATE XENON KINETIC MODEL

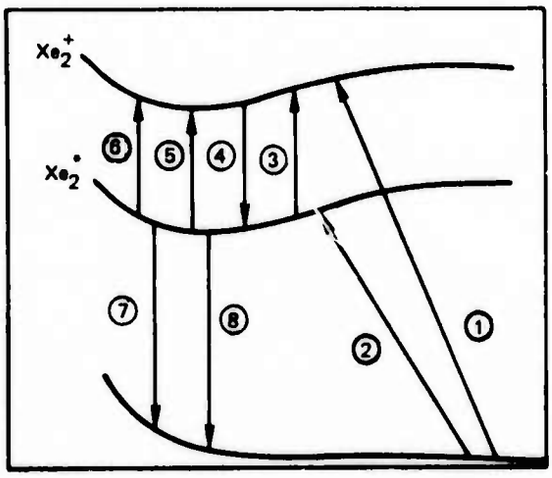

(1) $e + Xe^0 \longrightarrow Xe_2^+ + e + e$		(ELECTRON IMPACT)
(2) $e + Xe^0 \longrightarrow Xe_2^* + e$		(ELECTRON IMPACT)
(3) $e + Xe_2^* \longrightarrow Xe_2^+ + e + e$		(ELECTRON IMPACT)
(4) $e + Xe_2^+ \longrightarrow Xe_2^*$		(DISSOCIATIVE–RECOMBINATION)
(5) $Xe_2^* + Xe_2^* \longrightarrow Xe_2^+ + 2Xe + e$		(PENNING IONIZATION)
(6) $Xe_2^* + h\nu \longrightarrow Xe_2^+ + e$		(PHOTOIONIZATION)
(7) $Xe_2^* \longrightarrow 2Xe + h\nu$		(SPONTANEOUS EMISSION)
(8) $Xe_2^* + h\nu \longrightarrow 2h\nu + 2Xe$		(STIMULATED EMISSION)

N09-238-20

where (Xe^o) is the atomic ground state density, σ_{STE} is the cross section for stimulated emission, and the rate coefficients k_i refer to the processes in Fig. II-1. In these equations, the condition $[e] = [Xe_2^+]$ has been used. Processes (6) and (8) have cross sections of 10^{-19} cm^2 and 3.5×10^{-18} cm^2 respectively (Ref. 6), and therefore process (6) can be neglected for the purpose of the present discussion. The rates k_4, k_5, and k_7 have been taken from Ref. 7, and the rates k_1, k_2, and k_3 have been calculated as discussed by George (Ref. 6) for a Maxwellin distribution of the electron velocities. These rates are strong functions of the electron energy $\bar{u}_e$, which is related to the 10.6μ pumping intensity by the electron energy equation

$$\frac{e^2 I \nu}{m_e \varepsilon_o c\,(\omega^2 + \nu^2)} = [Xe^o]\, k_1\, \varepsilon_{o+} + [Xe^o]\, k_2\, \varepsilon_{o*} + [Xe_2^*]\, k_3\, \varepsilon_{*+}. \qquad (3)$$

In this equation, the term on the left is the inverse bremsstrahlung heating process and the quantities ε_{o+}, ε_{o*}, and ε_{*+} are the energies associated with the collisional processes (1), (2) and (3) in Fig. II-1. In the left-hand term, e is the electronic charge, I is the 10.6μ laser intensity, ν is the electron-heavy particle momentum transfer collision frequency, m_e is the electron mass, ε_o is the free-space permittivity, c is the speed of light, and ω is the laser radiation angular frequency.

For a 10.6μ beam propagating through a partially ionized gas, the absorption length can be written

$$\ell_a = \frac{m_e\, \varepsilon_o\, c\,(\omega^2 + \nu^2)}{[e]\, e^2\, \nu}\,. \qquad (4)$$

In order to have efficient coupling from the 10.6μ field to the discharge, it is necessary to operate with values of [e] and ν such that ℓ_a is comperable to the appropriate dimension of the discharge. For most of the anticipated pumping geometries, the 10.6μ rays come in off-axis with respect to the uv laser axis, and the absorption length would be comparable to the transverse width w and height h of the discharge, and small compared with the discharge length L_d.

Some typical examples of OPEDL discharges in xenon will be given below. These examples show that for reasonable values of [e], ν (i.e., pressure) ℓ_a, and cavity parameters, the coupling between the 10.6μ field and the uv laser field is very efficient and effective.

2.2 Case 1 - Large system, No Optical Cavity, Quasi-Steady State

As an example of a fairly large system, consider xenon at 15 atm and an active discharge with the dimensions w = h = 2.0 cm and L_d = 80 cm. Setting ℓ_a = w = 2.0 cm ($\Rightarrow$ [e] = 3×10^{15} cm^{-3}) and I_{uv} = 0, Eqs. (1) and (2) can be solved in steady-state to yield $[Xe_2^*] = 3 \times 10^{16}$ cm^{-3} and $\bar{u}_e$ = 1.18 eV. Equation (3) then gives the corresponding value of $I_{10.6}$ as 1×10^7 W/cm^2. The corresponding value of small signal gain, $\alpha_o = [Xe_2^*]\ \sigma_{STE}$, is 0.12 cm^{-1}. Using the value $k_7 \approx 10^8$ sec^{-1}, corresponding to the discussion in Ref. 7, indicates that for these conditions spontaneous emission is the dominant excimer loss process, and the above conditions give a uv saturation intensity $I_{uv})_s = (h\nu)_{uv}\ k_7/\sigma_{STE}$ of 3.3×10^7 W/cm^2. These results show that such a system would be well-suited to operate as a uv power amplifier.

2.3 Case 2 - Large System, Optical Cavity, Quasi-Steady State

Consider the same conditions as in Section 2.1. but with an optical cavity having reflectivities R_1 = 0.40 and R_2 = 0.80. Under lasing contitions, the excimer density is given by the threshold condition

$$[Xe_2^*] = [Xe_2^*]_{Th} = \frac{1}{\sigma_{STE}\ 2\ L_d} \ln\left(\frac{1}{R_1 R_2}\right) = 7 \times 10^{14} cm^{-3}. \tag{5}$$

Again taking ℓ_a = 2.0 cm ($\Rightarrow$ [e] = 3×10^{-15} cm^{-3}), Eqs. (1) and (2) can be solved in steady-state to give $\bar{u}_e$ = 1.10 eV and $I_{uv} = 9.0 \times 10^8$ W/cm^2. Equation (4) then gives $I_{10.6} = 2 \times 10^7$ W/cm^2. The corresponding uv power (internal to the cavity) is $P_{uv} = I_{uv}$ wh = 3.6 GW. An upper limit on the rate of gas temperature rise can be obtained by assuming that all of the 10.6μ energy absorbed goes into gas heating, and gives dTg/dt $\approx$ 600°K/μsec. Thus, the quasi-steady solution is probably valid for time scales up to ~1.0 μsec.

2.4 Scaling and Efficiency Considerations

The above example shows that the OPEDL concept is adaptable to large systems (e.g., 3.6 GW in the uv with reasonable values of the other parameters). From a kinetics point of view, the major limitation on scaling appears to be matching the absorption length ℓ_a to the dimensions of the system. From Eq. (4), it can be seen that increasing ℓ_a implies operating at lower value of [e]. Fortunately, this is compatible with scaling, since a lower value of [e] corresponds to a lower value of $[Xe_2^*]$, i.e., small signal gain. In large system, it is desirable to reduce the small signal gain in order to avoid self-oscillation and super-fluorescence.

In order to examine the efficiency of conversion from 10.6μ radiation to uv radiation, it is useful to define a coupling efficiency η_c as

$$\eta_c \equiv \frac{\text{power coupled into uv field}}{\text{power coupled out of 10.6}\mu\text{ field}} \quad . \tag{6}$$

For conditions typical of those in paragraph 2.3 above, the excimer density is relatively low, the uv flux is high, and processes (3), (5), (6) and (7) in Fig. 1 are negligible. For this case, Eq.s (1), (2) and (3) can be used to write the coupling efficiency η_c as

$$\eta_c = \frac{(h\nu)_{uv}\ [k_1 + k_2]}{k_1\ \varepsilon_{o+} + k_2\ \varepsilon_{o*}} = \frac{0.59\ (1 + \rho_1)}{1 + 0.76\ \rho_1} \tag{7}$$

where $\rho_1 \equiv k_2/k_1$. Thus, the coupling efficiency is in the range $0.59 \leq \eta_c \leq 0.78$, with $\eta_c \approx 0.71$ being typical.

Equation (7) can be interpreted physically by referring to Fig. II-1. With inverse bremsstrahlung absorption, all of the 10.6μ energy absorbed goes into electron heating. At the high values of $\bar{u}_e$ of interest here, the dominant energy loss from the electrons is via processes 1 and 2. At the

same time, in steady-state and at high uv fluxes, the net rate of molecules out of the excited state system is due to stimulated emission and must equal the net rate in via electron collisions. Thus, the efficiency involves only the electron rates, multiplied by the appropriate energy. The excess energy, involved in the processes $Xe^* \rightarrow Xe_2^*$, $Xe^+ \rightarrow Xe_2^+$, and $Xe_2^+ \rightarrow Xe_2^*$ results primarily in gas heating. Because $(h\nu)_{uv} = 0.85\ \varepsilon_{o*}$ and $(h\nu)_{uv} = 0.59\ \varepsilon_{o+}$ for the xenon system, the coupling efficiency is potentially very high.

SECTION III

NUMERICAL MODELING STUDIES

3.1 Description of the Model

The discussion in Section II was based on an approximate model, which is valid at pressures above 10 atm. As will be discussed later, preliminary experiments indicate that operation at somewhat lower pressures and operation with a helium buffer gas enhance the uniformity of the optically-pumped discharge. In order to model such conditions accurately, the kinetic model shown in Figs. III-1, and in Tables III-1 and III-2 was developed. Rate equations for the various species, analogous to the equations in Section II, are integrated forward in time, starting from a set of intitial conditions corresponding to some initial level of preionization. The 10.6μ intensity as function of time is an input quantity. In addition to the parameters mentioned in Section II, a total efficiency η_T defined as

$$\eta_T \equiv \frac{(R_1 - R_2)\, R_2}{R_1 + R_2} \quad \frac{\int_o^t I_{uv}(\tau)\, wh\, d\tau}{\int_o^t I_{10.6}(\tau)\, h\, L_d\, d\tau},$$

is calculated, and approximates the uv radiation actually coupled out of the uv cavity, as well as accounting for the fact that in a pulsed system, the efficiency based on total energy is a better measure of performance than the instantaneous coupling efficiency.

In order to check the validity of the computer model, cases were run corresponding to the afterglow plasma produced by a short pulse E-beam. Input values of the various species were taken from Ref. 7, and the concentrations of the various species (in the absence of an optical cavity) were calculated for times up to 250 nsec following the E-beam pulse. Good agreement with Ref. 7 was obtained for pressures from 1.4 atm to 42.5 atm.

SCHEMATIC ENERGY LEVEL DIAGRAM FOR XENON

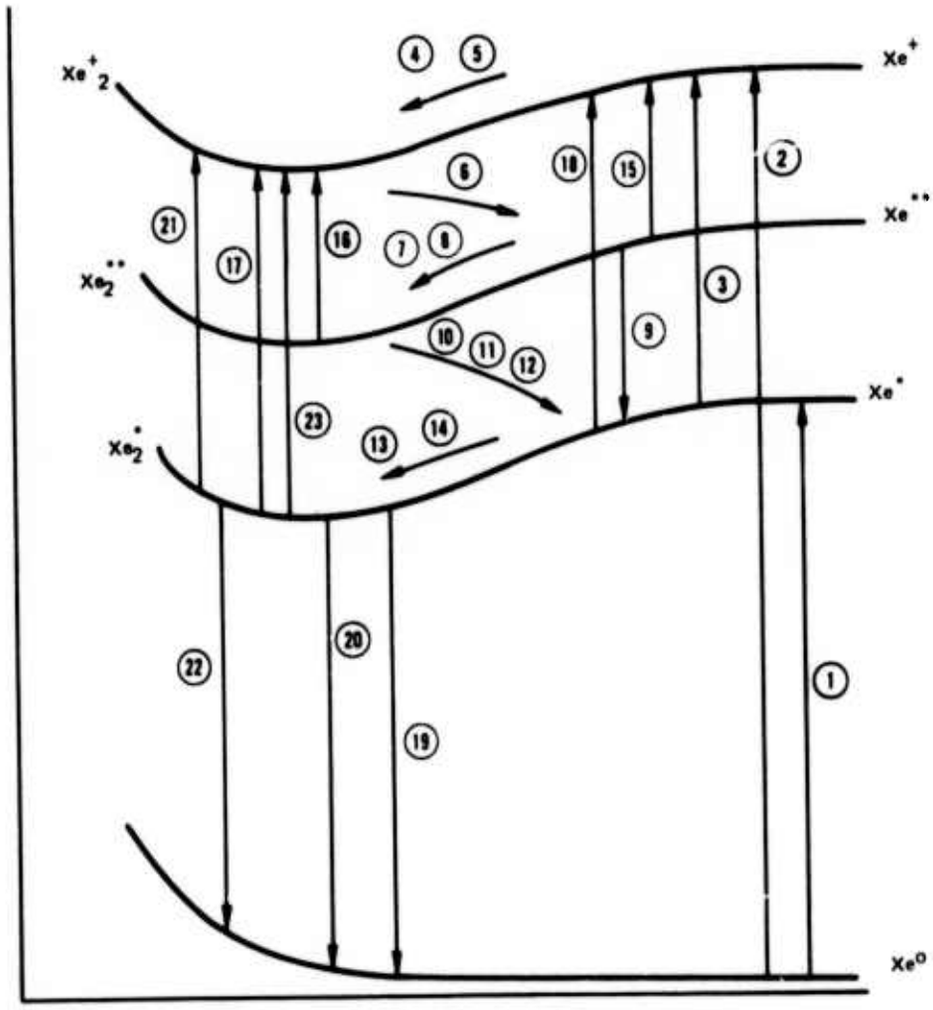

TABLE III-1.

Kinetic Processes Treated in Numerical Model

$$e + Xe^{o} \rightarrow Xe^{*} + e \quad (1)$$

$$e + Xe^{o} \rightarrow Xe^{+} + e + e \quad (2)$$

$$e + Xe^{*} \rightarrow Xe^{+} e + e \quad (3)$$

$$Xe^{+} + 2Xe \rightarrow Xe_2^{+} + Xe \quad (4)$$

$$Xe^{+} + Xe^{o} + He^{o} \rightarrow Xe_2^{+} + He^{o} \quad (5)$$

$$Xe_2^{+} + e \rightarrow Xe^{**} + Xe^{o} \quad (6)$$

$$Xe^{**} + 2Xe^{o} \rightarrow Xe_2^{**} + Xe^{o} \quad (7)$$

$$Xe^{**} + Xe^{o} + He^{o} \rightarrow Xe_2^{**} + He^{o} \quad (8)$$

$$Xe^{**} \rightarrow Xe^{*} + h\nu \quad (9)$$

$$Xe_2^{**} + Xe^{*} \rightarrow Xe^{*} + 2Xe^{o} \quad (10)$$

$$Xe_2^{**} + He^{o} \rightarrow Xe^{*} + Xe^{o} + He^{o} \quad (11)$$

$$Xe_2^{**} + e \rightarrow Xe_2^{*} + e \quad (12)$$

$$Xe^{*} + 2Xe \rightarrow Xe_2^{*} + Xe \quad (13)$$

$$Xe^{*} + Xe + He \rightarrow Xe_2^{*} + He \quad (14)$$

$$Xe^{**} + Xe^{**} \rightarrow Xe^{+} + Xe + e \quad (15)$$

$$Xe_2^{**} + Xe_2^{**} \rightarrow Xe_2^{+} + 2Xe + e \quad (16)$$

$$Xe_2^{*} + Xe_2^{*} \rightarrow Xe_2^{+} + 2Xe + e \quad (17)$$

$$Xe^{*} + Xe^{*} \rightarrow Xe^{+} + Xe + e \quad (18)$$

$$Xe_2^{*} + e \rightarrow 2Xe + e \quad (19)$$

$$Xe_2^{*} \rightarrow 2Xe + h\nu \quad (20)$$

Table III-1 (Con't)

$$Xe_2^* + h\nu \rightarrow Xe_2^+ + e \quad (21)$$

$$Xe_2^* + h\nu \rightarrow 2h\nu + 2Xe \quad (22)$$

$$e + Xe_2^* \rightarrow Xe_2^+ + e + e \quad (23)$$

Table III-2.

Rates Used in Numerical Model

Process	Rate	Data Source
1	Note 1	Refs. 8,9
2	Note 2	Refs. 8, 9
3	Note 3	Refs. 9, 10
4	2.5×10^{-31} cm^6/sec	Ref. 7
5	1.0×10^{-31} cm^6/sec	Ref. 7
6	2.0×10^{-7} cm^3/sec	Ref. 7
7	1.0×10^{-31} cm^6/sec	Ref. 2
8	1.0×10^{-31} cm^6/sec	Estimate based on Ref. 2
9	1.5×10^{7} sec^{-1}	Ref. 2
10	1.0×10^{-11} cm^3/sec	Ref. 2
11	1.0×10^{-11} cm^3/sec	Estimate based on Ref. 2
12	1.0×10^{-6} cm^3/sec	Ref. 2
13	5.0×10^{-32} cm^6/sec	Ref. 2
14	2.0×10^{-32} cm^6/sec	Estimate based on Ref. 2
15	5.0×10^{-10} cm^3/sec	Ref. 2.
16	5.0×10^{-10} cm^3/sec	Ref. 2
17	5.0×10^{-10} cm^3/sec	Ref. 2
18	5.0×10^{-10} cm^3/sec	Ref. 2
19	1.0×10^{-9} cm^3/sec	Ref. 2
20	5.0×10^{7} sec^{-1}	Ref. 2
21	$Q_p = 1.0 \times 10^{-19}$ cm^2	Cross section inferred from Ref. 11
22	$Q_{STE} = 7.0 \times 10^{-19} cm^2$	Ref. 11
23	$k_{23} = k_3$	

Note 1 : Rate obtained by integrating the cross section over a Maxwellian distribution function. The peak cross section value was estimated as 4×10^{-16} cm^2 based on data for Argon in Ref. 8, and the cross section shape was assumed to be that derived in Ref. 9.

Note 2: Rate obtained by integrating the cross section over a Maxwellian distirbution function. The peak cross section value was estimated as 0.40×10^{-16} cm^2 based on the data for Argon in Ref. 8, and the cross section shape was assumed to be that derived in Ref. 9.

Note 3: Rate obtained by integrating the cross section over a Maxwellian distribution function. The peak cross section value was estimated as 1.0×10^{-15} cm^2 by analogy to Cs and based on the data for Cs in Ref. 10. The cross section shape was assumed to be that derived in Ref. 9.

3.2 Typical Results

Typical results obtained with the numerical code are shown in Figs. III-3 - III-6. The values of the various input parameters are listed on the figures.

Figure III-3 shows results corresponding to a small system operating at a fairly low xenon pressure, such as might be encountered in the small scale experiments to be described later. These results show that using a max R mirror (~ 88% reflecting @ 1730Å) and a 7% output coupling mirror, the system reaches lasing threshold and produces an output laser pulse which should be easily detectable. The pumping 10.6μ pulse shape was taken as that typical of a gain-switched TEA laser. Because of the low output coupling, the total efficiency η_T for this case is rather low.

Figure III-4 shows a similar calculation but for a much larger system and with a slightly shorter pumping pulse. For this case, in order to keep ℓ_a large, corresponding to the larger system, the 10.6μ peak intensity was reduced (3×10^7 W/cm^2 vs. 8×10^7 W/cm^2 in Fig. III-3). The peak uv intensity is somewhat lower than for the small system; however, the coupling efficiency is slightly higher (62% vs 52%) and the total efficiency is much higher (19% vs 2%). This case illustrates some of the scaling effects discussed in Section II, and shows that the overall efficiency, even in a pulsed system utilizing the pulse shape from a conventional TEA laser, can be very high.

The numerical code was used to obtain quasi-steady-state results by using a 10.6μ pumping pulse with a flat portion, and the results are shown in Fig. III-5. These results show that the electron density [e] and the uv intensity I_{uv} (as well as the various species concentrations) come into equilibrium with the pumping radiation on a time scale of ~10 nsec. As expected, the gas temperature rises linearly during the quasi-steady portion of the pulse; and, since the system is in the optimum coupling range for a longer fraction of the pumping pulse, the total efficiency η_T reaches a higher value than in Fig. III-4.

Figure III-5 is a simulation of conditions in which the electron density [e] starts out at a very high value. This case corresponds to the use of a short-pulse electron beam to produce the initial ionization, with the bulk of the pumping energy provided by the 10.6μ beam. It can be seen that the results are very similar to those in Fig. III-4. From a practical viewpoint however, the use of an electron beam for preionization might have advantages in terms of discharge uniformity and stability.

FIG. III-2

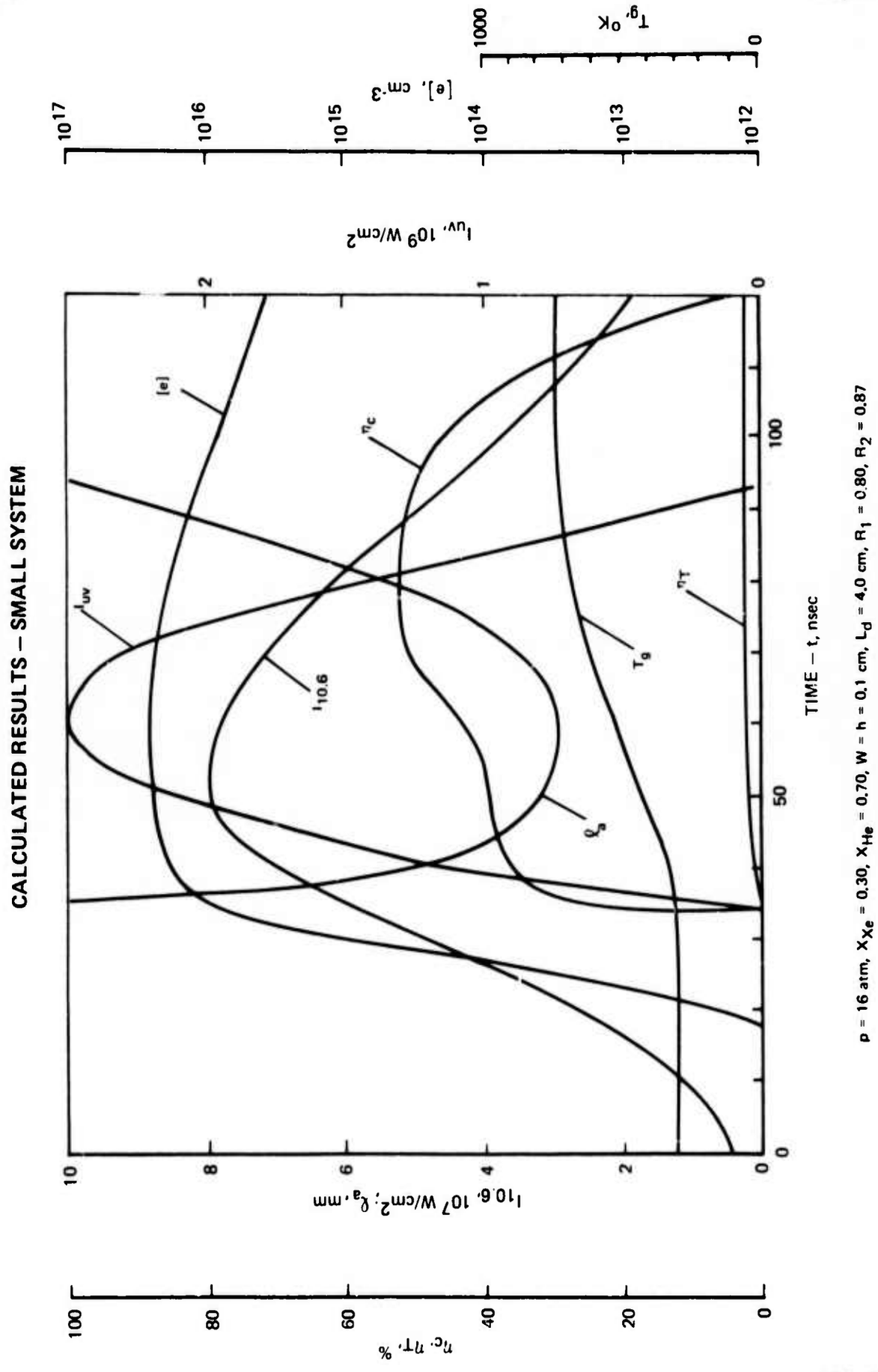

N09-238-1

FIG. III-3

CALCULATED RESULTS – LARGE SYSTEM

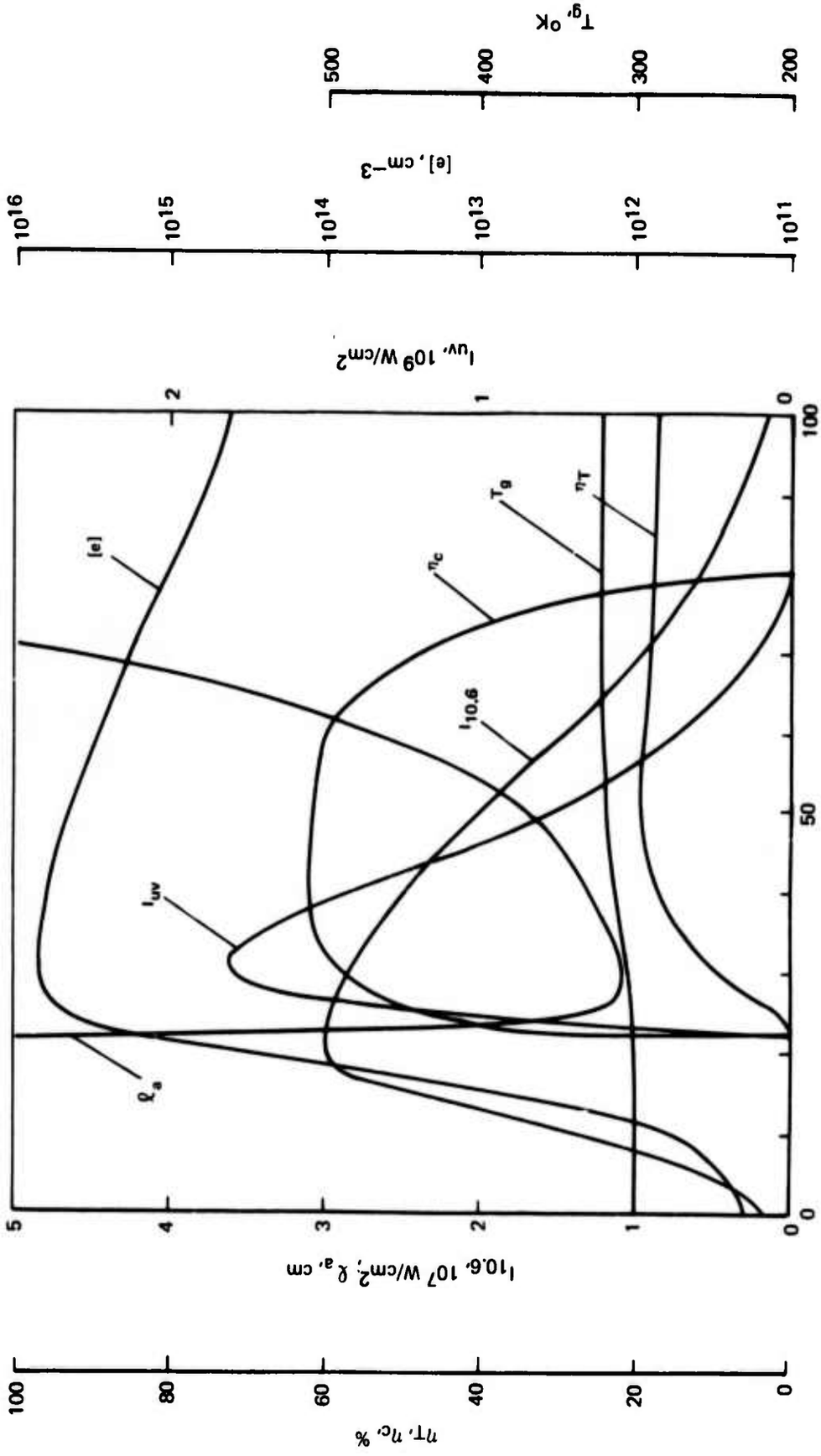

p = 16 atm, X_{Xe} = 1.0, w = h = 1.0 cm, L_d = 100 cm, R_1 = 0.20, R_2 = 0.88

N09-238-27

FIG. III-4

CALCULATED RESULTS – QUASI-STEADY STATE

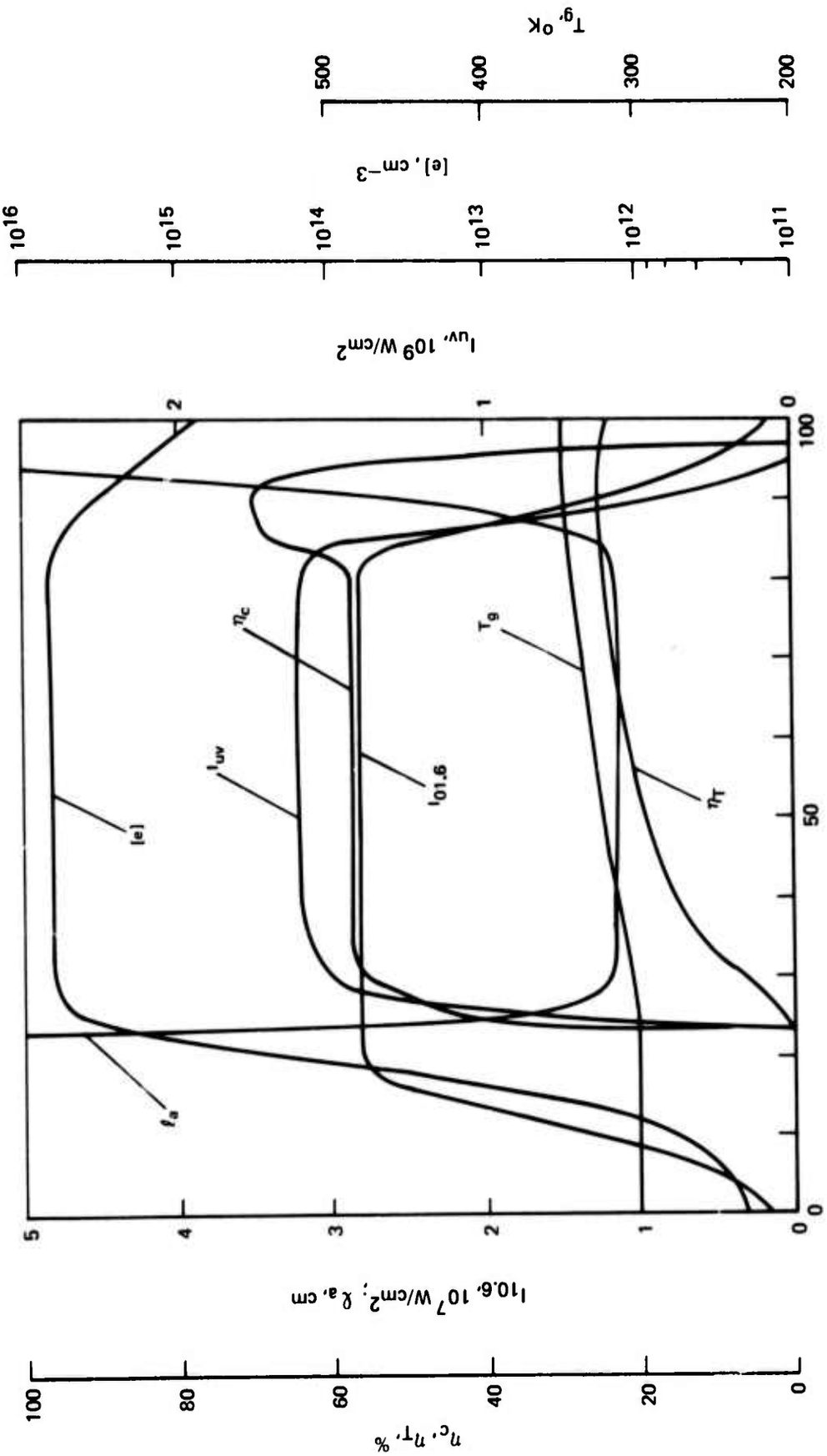

p = 16 atm, X_{Xe} = 1.0, w = h = 1.0 cm, L_d = 100 cm, R_1 = 0.20, R_2 = 0.88

N09-238-3

FIG. III-5

CALCULATED RESULTS — HIGH INITIAL ELECTRON DENSITY

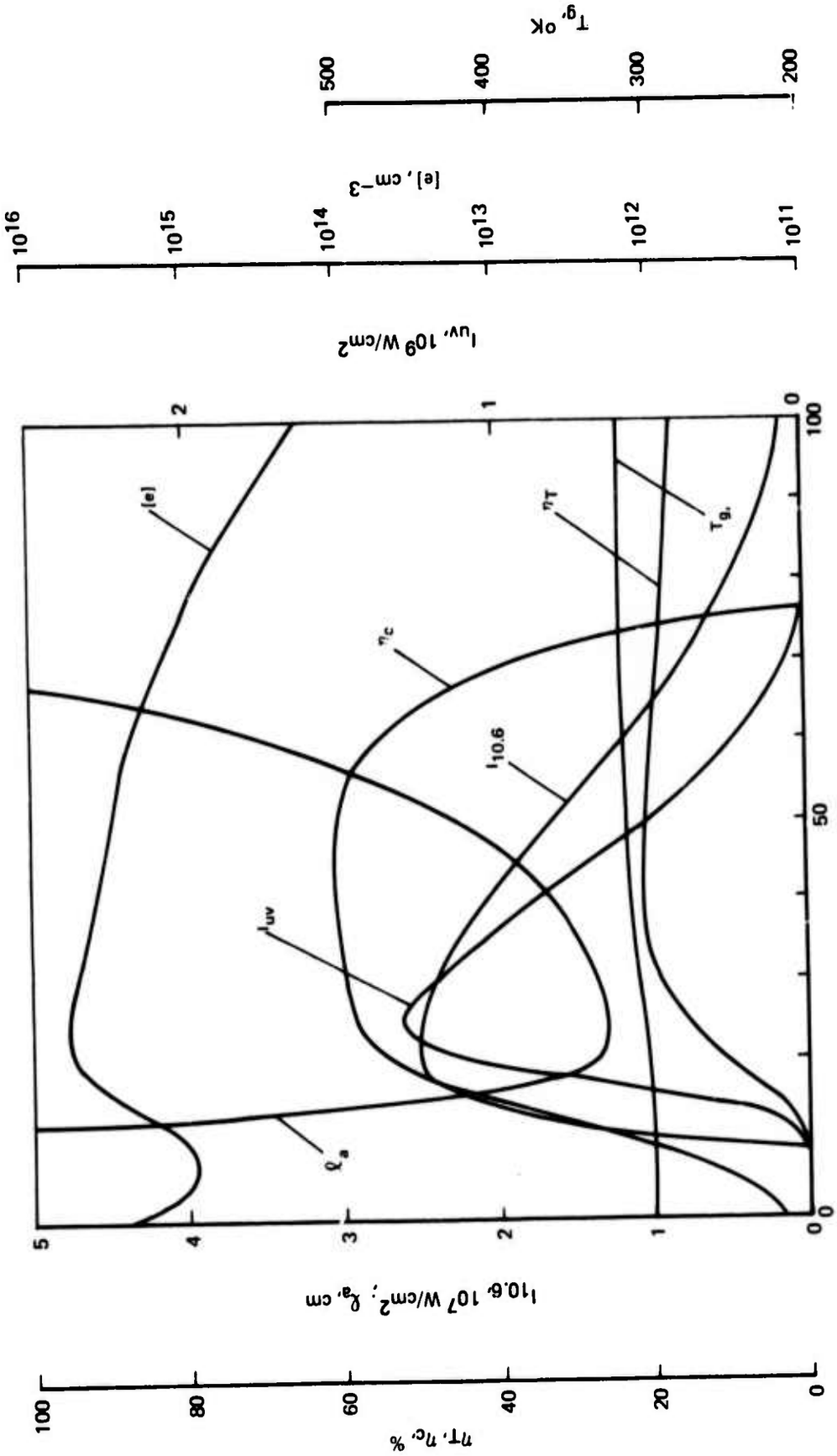

p = 16 atm, X_{Xe} = 1.0, w = h = 1.0 cm, L_d = 100 cm, R_1 = 0.20, R_2 = 0.83

N09-238-2

SECTION IV

EXPERIMENTAL FACILITY

4.1 TEA Laser

Previous experience[12] indicated that in order to obtain good results with the optically-pumped discharge technique, it is necessary to have a pumping laser with good beam quality, pulse-to-pulse repeatability, long-term stability, and flexibility. This is particularly true when working with noble gases at high pressures.

During this report period, considerable effort was expended in upgrading the CO_2 laser facility. The entire experiment was moved to a larger laboratory, and the various elements of the optical train were mounted on a stable optical table. In the previous setup, the system tended to drift out of alignment due to changes in the ambient temperature of the room and due to the heat generated by the electronics. In the present setup, these problems have been eliminated.

A diagram of the TEA laser is shown in Fig. IV-1. Several of the components can be seen in the photograph of the experiment in Fig. IV-2. The oscillator is a helical-pin TEA laser,[13] with an internal aperture to obtain fundamental mode operation and with a 35% reflecting output mirror. This laser produces 0.5 J when operated with a $He/N_2/CO_2$ mixture, with 80% of the energy occuring in the gain-switched leading spike of the pulse; and produces 0.1 J when operated with a He/CO_2 mixture, with 100% of the energy occurring in the gain-switched spike. The laser tends to be self mode-locked (i.e., the pulse consists of a series of short spikes within the gain-switched pulse envelope), particularly when operated without nitrogen.

The amplifier is a 3-pass TEA discharge based on the design described by Pan,[14] and provides $\sim$ 20 dB of amplification. The system generates pulses with peak powers in excess of 100 MW and produces gas breakdown spots in air over a 1.0 m length when focused with a 2.5 m focal length mirror. By varying the charging voltage on the amplifier capacitors and by varying the reflectivity of the mirror R_{10} in Fig. IV-1, the laser intensity at the test cell can be varied by approximately a factor of twenty without significantly changing the other properties (e.g., pulse shape, divergence, transverse profile, etc.) of the beam.

A typical beam burn pattern at the exit of the amplifier is shown in Fig. IV-3-a along with a gold-doped germanium detector trace of the pulse shape in Fig. IV-3-b. In this trace, the oscillator was operated with $He/N_2/CO_2$.

FIG. IV-1

DIAGRAM OF TEA LASER SYSTEM

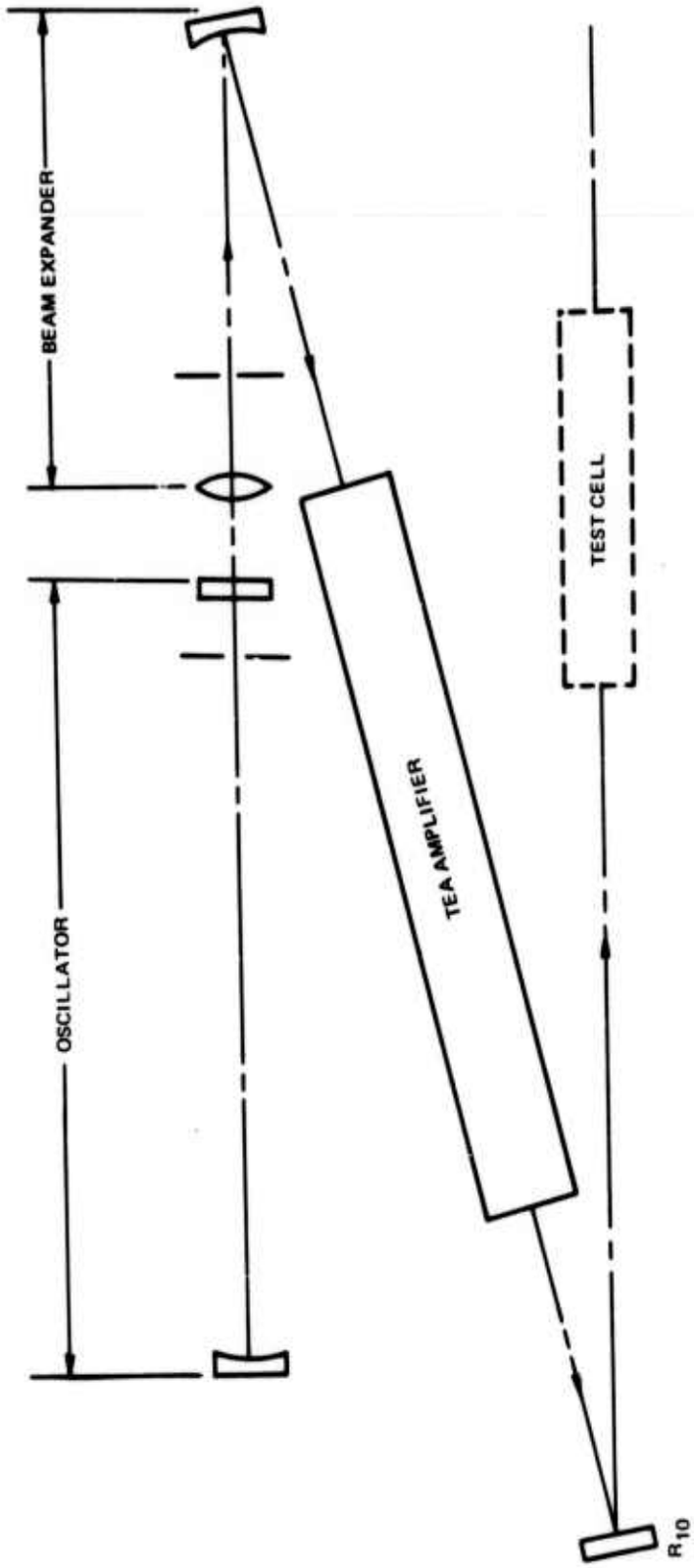

N09-238-19

PHOTOGRAPH OF EXPERIMENT

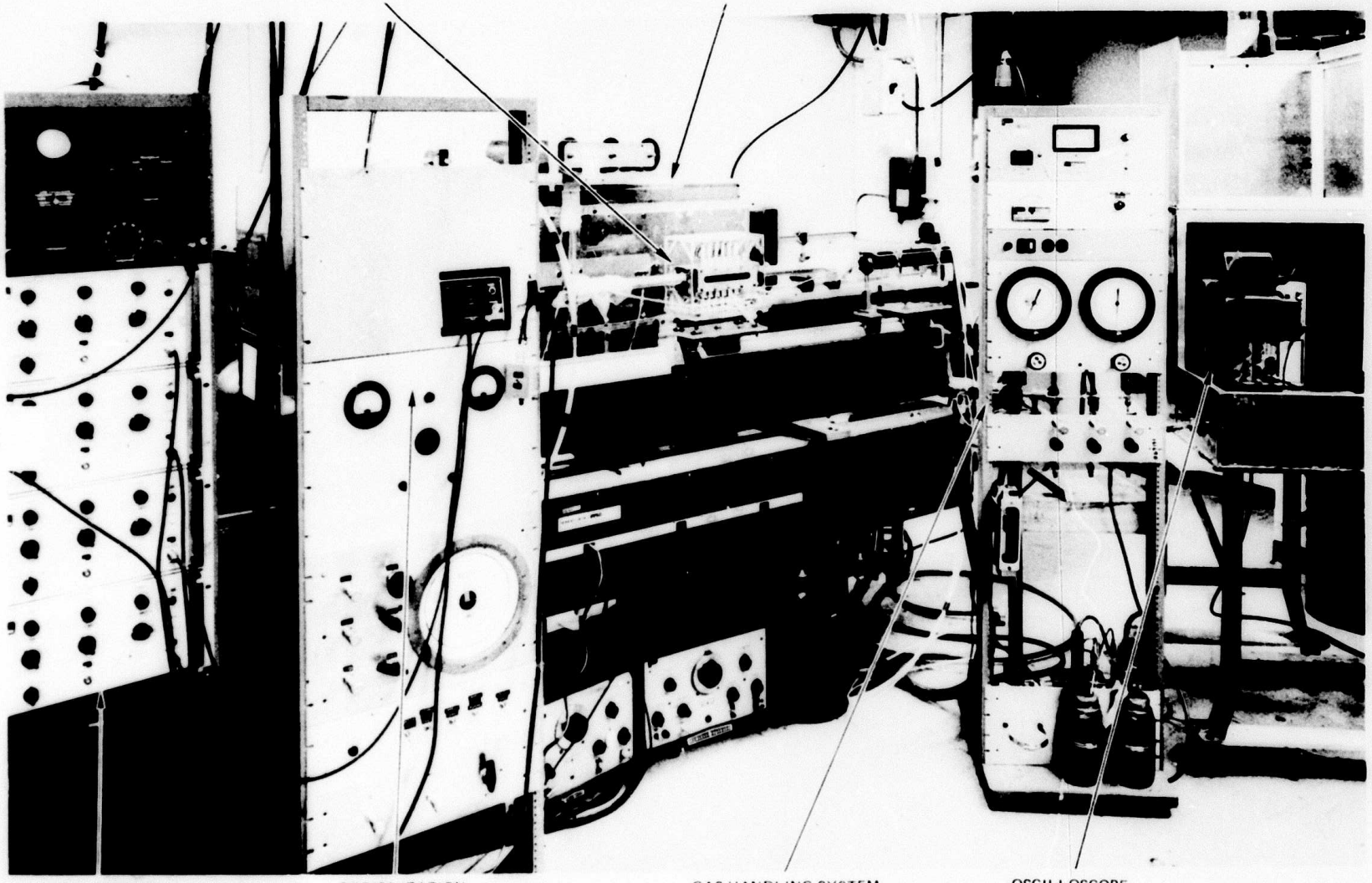

FIG. IV-2

a. NEAR FIELD LASER BURN PATTERN

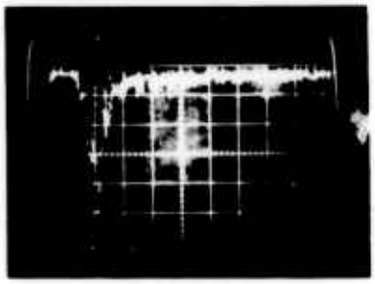

200 nsec/div

b. TEA LASER PULSE SHAPE

4.2 Gas Handling System

The gas handling system for pumping the test cell down to 10^{-6} torr and back-filling it with high-purity, filtered gas up to 20 atm is shown in Fig. IV-2. This system uses either a liquid-nitrogen - trapped mechanical pump or an adsorption pump for roughing and a vacion pump for final pumping. The high-pressure side of the system can also be used to operate the cell in an open-flow configuration with the cell operating at high pressure, but with the gas exhausting from the cell into the lab. (This latter mode is not practical with xenon, but is very useful when running $He/N_2/Ar$ mixtures).

4.3 Test Cells

During this report period, two test cells were designed and fabricated. The first cell, which can be seen mounted on the optical rail in Fig. IV-2, is a high-aspect-ratio cell. This cell was designed to study the discharge kinetics at high pressure using an optical configuration with known properties.[12] The preionization was produced by two rows of spark plugs which were designed and fabricated to operate under the stringent requirements of cleanliness, high vacuum, and high pressure of interest here.

A second cell, designed to utilize the optical configuration sketched in Fig. IV-4, was also fabricated and is shown in Fig. IV-5. The preionization spark plugs are the same as those used in cell #1.

4.4 Diagnostics

In order to monitor the uv and visible radiation of interest, several diagnostic systems have been fabricated. The primary measuring device is a photodetector mounted in a double-shielded box as shown in Fig. IV-5. The signals are recorded using a Tektronix 7904 oscilloscope. The scope along with the biasing supply for the photodetector are mounted in an isolation cage, as shown in Fig. IV-2. This system has the sensitivity and time response to provide accurate signals with good signal-to-noise ratio, even in the high noise environment of the large TEA laser in use as the pumping source. The other diagnostics in use consist of spectrographs and spectrometers, as well as a conventional camera to photograph the optically-pumped discharge.

TRANSVERSE PUMPING CONFIGURATION

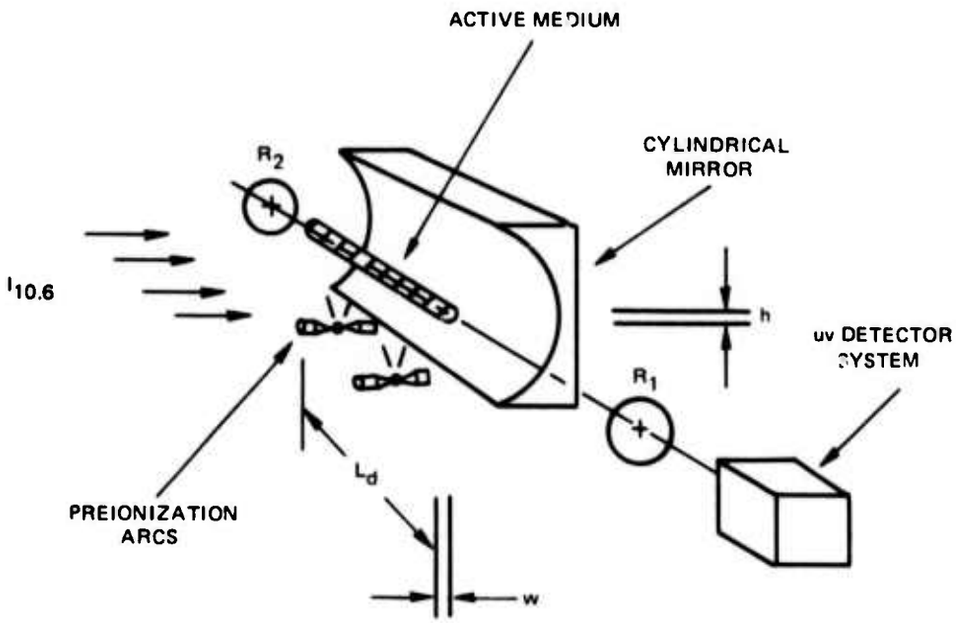

FIG. IV-5

PHOTOGRAPH OF TRANSVERSE PUMPING CELL

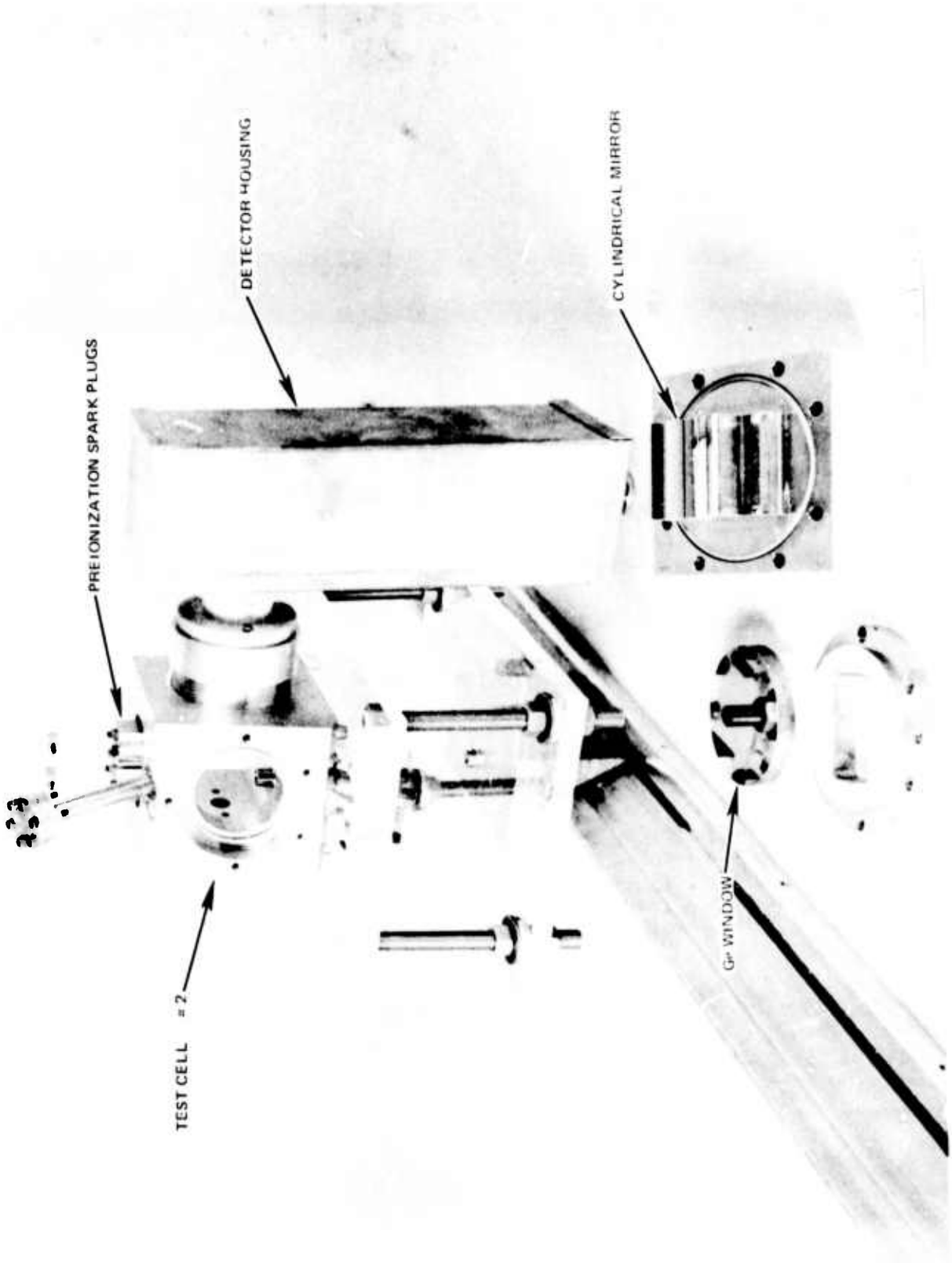

N09 238 14

SECTION V

EXPERIMENTAL RESULTS

5.1 Introduction

In Sections III and IV, theoretical calculations were carried out for high-pressure mixtures of He/Xe. These studies showed that the optically-pumped discharge technqiue is capable of producing a highly efficient laser operating on the 1730Å transition in molecular xenon. In these calculations, it was assumed that the discharge was uniform and diffuse over the volume being considered. In the preliminary experiments to be described here, it was found that operation of a diffuse discharge in a mixture of He/Xe at 16 atm was not possible. This result appeared to be due to the presence of aerosols in the cell, which caused breakdown spots in the focal volume, rather than a diffuse discharge. This effect is illustrated in Fig. V-1. Figure V-1-b shows a diffuse discharge obtained by evacuating the cell and back-filling it to 5.0 atm with 7% N_2, 93% He. From the photo it can be seen that the focal diameter is ~ 0.1 cm, and it should be noted that the intensity of 6.0×10^8 W/cm^2 is above the threshold for breakdown in "lab air" at 5.0 atm[15] for a focal diameter of 0.1 cm. Figure V-1-c shows the discharge obtained when the conditions in Fig. V-1-b were repeated, but with the same gas fill. It can be seen that there are multiple breakdowns in the focal volume caused by aerosols. It was determined that under some conditions the primary sources of aerosols were the preionization arcs, probably from sputtering at the preionization electrodes. In other cases, the aerosols appeared to be due to insufficient cleaning of the cell, cell windows, and gas fill lines. It was found that under many conditions the aerosols could be reduced to an acceptable level either by flowing the working gas continuously through the cell and waiting several seconds between shots, or by pumping the cell out and back-filling it with clean gas between shots.

5.2 Coaxial Discharge Studies at High Pressure

A large number of discharge photographs were taken under various conditions, in order to determine under what conditions diffuse discharges could be obtained. Figure V-2 shows a series of shots in He/N_2 mixtures at high pressures. Figures V-2-b and V-2-d correspond to a slight reduction in X_{N_2} and a slight increase in I_o respectively, and illustrate discharges which are just on the verge of breaking down during the pulse. It should be noted that these breakdowns are due to over-driving the discharge, rather than to aerosols, and are qualitatively different from that in Fig. V-1-c. The existence of the near breakdown in Fig. V-1-d (caused by the absorption length ℓ_a becoming small compared to the focal volume length) indicates that in Fig.

OPTICALLY-PUMPED DISCHARGES IN He/N_2

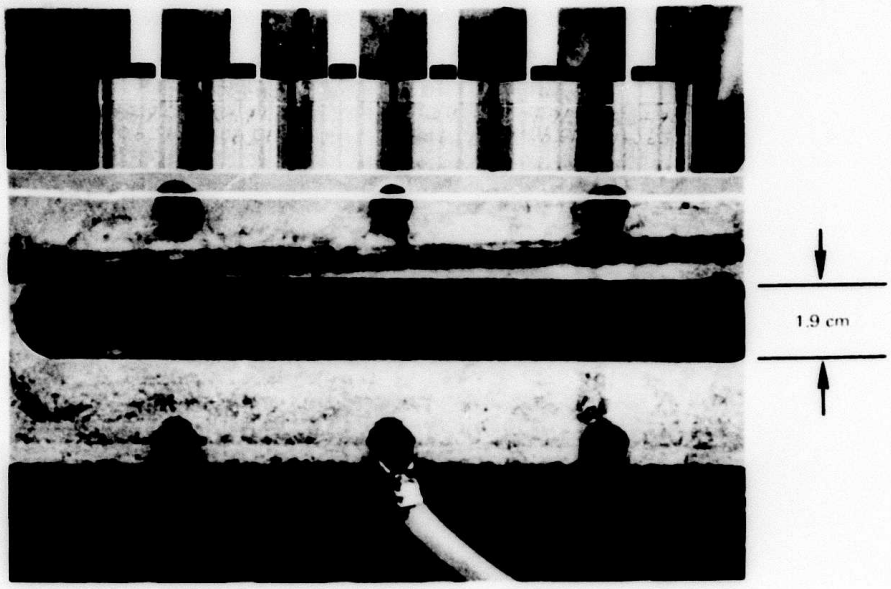

a. TEST CELL

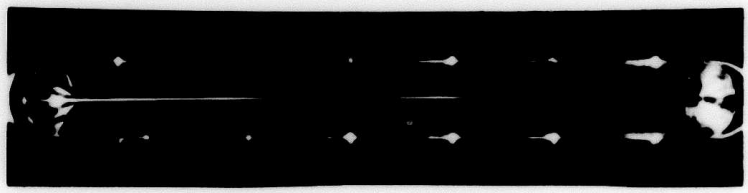

b. DIFFUSE DISCHARGE, $p = 5.0$ atm, $X_{N_2} = 0.07$, $X_{He} = 0.93$, $I_o = 6.0 \times 10^8$ W/cm^2

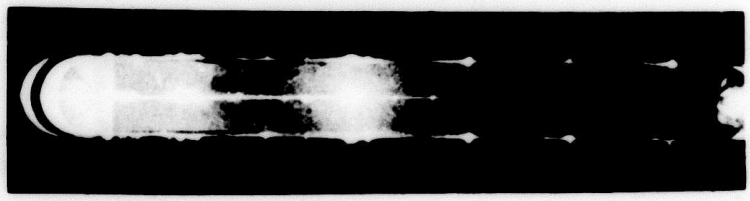

c. AEROSOL-INDUCED BREAKDOWN, $p = 5.0$ atm, $X_{N_2} = 0.07$, $X_{He} = 0.93$

$I_o = 6.0 \times 10^8$ W/cm^2

NOD 238 13

OPTICALLY-PUMPED DISCHARGES IN He/N_2

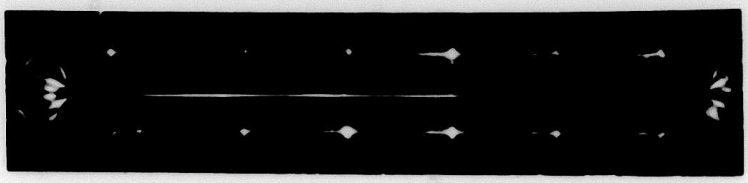

a. $p = 7.1$ atm, $X_{N_2} = 0.14$, $X_{He} = 0.86$, $I_o = 8.0 \times 10^8$ W/cm^2

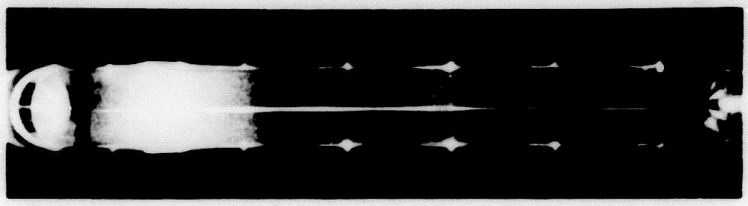

b. $p = 7.1$ atm, $X_{N_2} = 0.12$, $X_{He} = 0.88$, $I_o = 8.0 \times 10^8$ W/cm^2

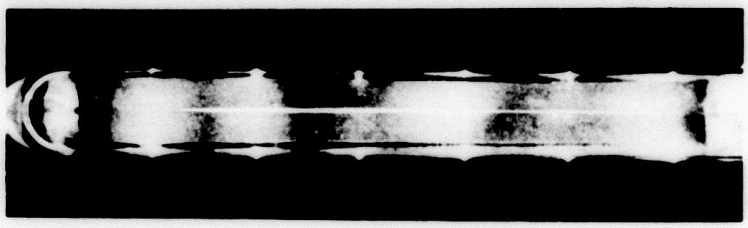

c. $p = 12.0$ atm, $X_{N_2} = 0.13$, $X_{He} = 0.87$, $I_o = 6.0 \times 10^8$ W/cm^2

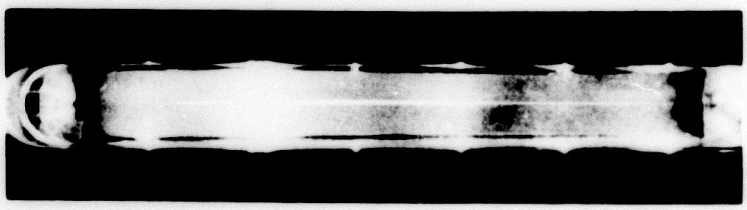

d. $p = 12.0$ atm, $X_{N_2} = 0.13$, $X_{He} = 0.87$, $I_o = 7.0 \times 10^8$ W/cm^2

N09-238-23

V-2-c the absorption length ℓ was $\ell_a \approx 10$ cm. From Eq. (5), and for the gas mixture and pressure in Fig. V-2-c, we can infer an electron density $[e] \approx 2 \times 10^{15} cm^{-3}$. Thus the sequence of photos in Fig. V show that it is possible to obtain high-pressure, high-electron density, diffuse discharges using the optical pumping technique.

Figure V-3 shows discharges in mixtures of $He/Ar/N_2$. In the presence of Ar, the preionization arcs are very bright and tend to saturate the film, causing the rather poor quality of the photos. However, viewing the original photos and visual observation of the discharge showed that there were no breakdowns present, and thus Fig. V-3-b demonstrates a diffuse discharge in $He/Ar/N_2$ at 15 atm.

Figure V-4 shows a discharge in He/Ar at 2.0 atm. Since the kinetics of He/Ar are very similar to those of He/Xe, this photo (which was obtained near the end of the reporting period) represents a step toward achieving discharges in He/Xe mixtures at several atmospheres.

5.3 Transverse Pumping Studies

As described in Section IV a test cell was fabricated which utilized a cylindrical mirror to focus the 10.6μ radiation along a line. The objective was to generate an optically pumped discharge along this line, and to place the uv mirrors around this discharge as shown in Fig. IV-4. Unfortunately, attempts to operate with this configuration were unsuccessful, due to the formation of breakdown spots in the focal volume.

Typical discharge photos are shown in Fig. V-5. These photos are somewhat difficult to interpret due to the various reflections from the cylindrical mirror. (The bright lines in Fig. V-5-a are reflections from the preionization arcs). Figure V-5-f was obtained by increasing the pumping intensity to a value well above threshold and stopping the camera down to avoid saturation of the film. It was determined that the breakdowns were due to over-driving the discharge, rather than to aerosols in the cell (When the preionization arcs were turned off, no breakdown occurred). Apparently the transverse structure in the beam profile (see e.g., Fig. IV-3-a) along with the low effective f number of the mirror (~2.0 cm f.l.) caused hot spots at the focus which were severe enough to cause breakdown at these spots before other portions of the discharge could reach a significant level of ionization.

Because of the obvious non-uniformity of the discharge, no attempts were made to operate this cell with uv mirrors.

OPTICALLY–PUMPED DISCHARGES IN $He/Ar/N_2$

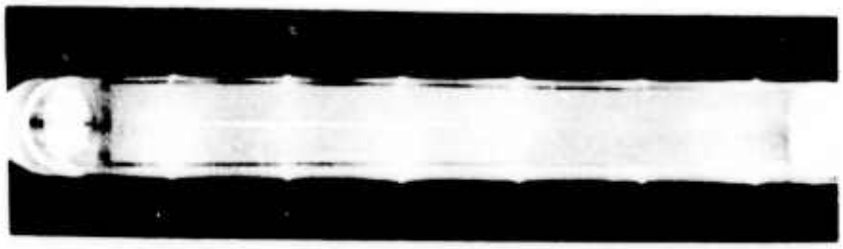

a. $p = 10.0$ atm, $X_{N_2} = 0.10$, $X_{Ar} = 0.50$, $X_{He} = 0.40$, $I_o = 4.2 \times 10^8$ W/cm^2

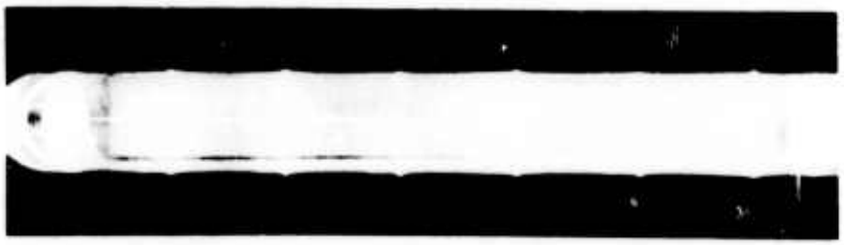

b. $p = 15.0$ atm, $X_{N_2} = 0.10$, $X_{Ar} = 0.50$, $X_{He} = 0.40$, $I_o = 6.0 \times 10^8$ W/cm^2

N09–238–7

OPTICALLY–PUMPED DISCHARGE IN He/Ar

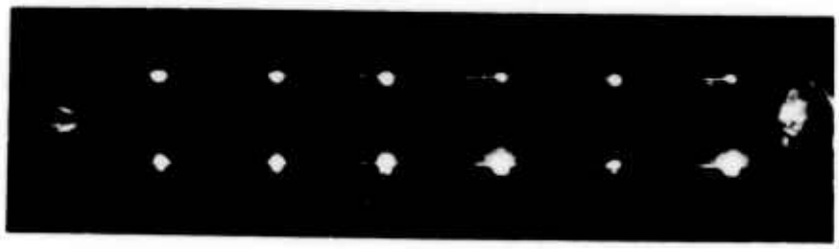

$p = 2.0$ atm, $X_{He} = 0.50$, $X_{Ar} = 0.50$, I_o 1×10^8 W/cm^2

TRANSVERSE PUMPING PHOTOS

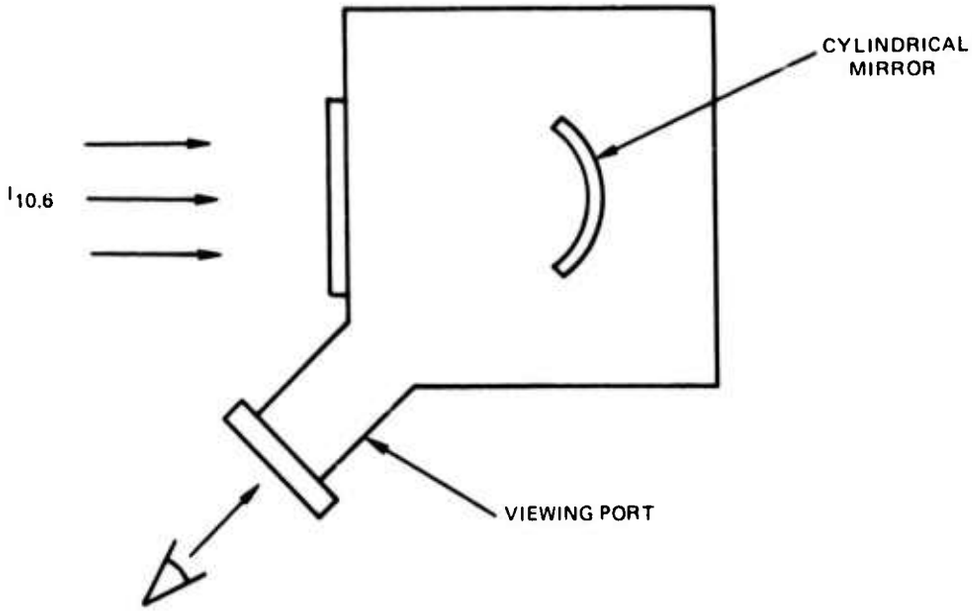

a. DIAGRAM OF VIEWING ARRANGEMENT

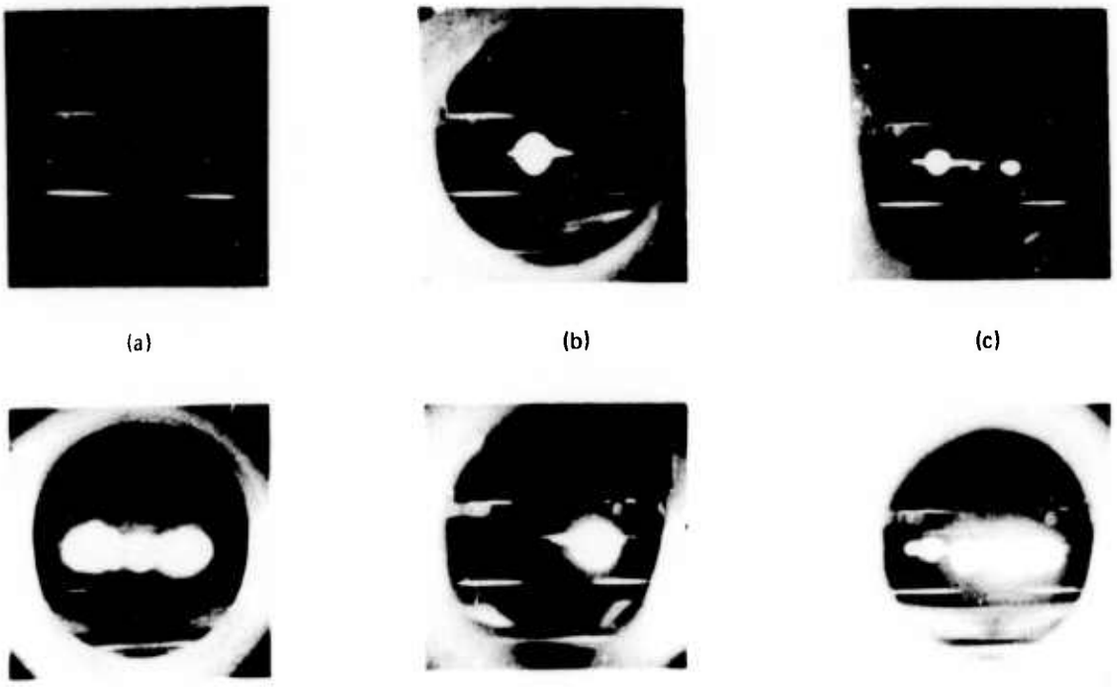

N09-238-6

5.4 Kinetic Studies

Because of the success with $He/Ar/N_2$ mixtures, described in Section 5.2, and because of the reported success with the electron-beam pumped Ar/N_2 excimer system[3], studies were carried out to investigate whether the excimer transfer process was taking place in the optically pumped discharges.

A photodetector with a narrow-band filter (50 Å hw) at 3371 Å was used to monitor the spontaneous emission from the optically-pumped discharge under a variety of conditions. Under non-lasing conditions, the intensity of this emission is proportional to the population of the $C^3\pi$ state of molecular nitrogen and the decay time of the spontaneous emission signal gives information regarding the population and depopulation of this state. The measurements were carried out using cell #1, and the discharge was viewed end-on through a sodium-chloride window.

In carrying out these tests, a very interesting effect was noted and is shown in Fig. V-6. As mentioned in Section IV, the oscillator tends to be self-mode locked. It was found that at nitrogen partial pressures $p_{N_2} \gtrsim 0.3$ atm, the 3371 Å spontaneous emission signal showed the same spiked profile shape as the 10.6μ laser pulse. The two bottom traces in Fig. V-6 were taken with no N_2 in the 10.6μ oscillator and correspond to a strongly self-mode-locked condition. These traces clearly show that the spontaneous-emission decay time for these conditions was $\tau_d < 5$ nsec, which is consistent with the nitrogen self-quenching rate quoted in Ref. 3.

Figure V-7 shows the spontaneous emission trace for a case in which the nitrogen self-quenching time ($\tau_q \approx 180$ nsec, based on the rate $k_q = 1.1 \times 10^{-11}$ cm^3/sec, quoted in Ref. 3) is long compared to the spontaneous decay time of 40 nsec. For this case, the spontaneous decay rate dominates, and the decay time is equal to the spontaneous decay time.

Figure V-8 shows a sequence of spontaneous emission traces in $He/Ar/N_2$, for various nitrogen fractions. In Fig. V-8-a, the decay time is approximately equal to the nitrogen self-quenching time of ~ 30 nsec. As the nitrogen fraction is reduced, with a corresponding increase in the self-quenching time, the decay time increases, reaching a value of ~ 500 nsec in Fig. V-8-d. This time is much longer than the 40 nsec spontaneous decay time and is much longer than the 150 nsec 10.6μ pumping pulse time, indicating that significant energy transfer occurs from the argon excimers to the $C^3\pi$ nitrogen state in the afterglow plasma. This effect is similar to that observed in electron-beam-pumped discharges[16] and indicates that the optically-pumped discharge in high-pressure $He/N_2/Ar$ should posess the same attractive efficiency of kinetic coupling as the electron-beam lasers.

3371 Å SPONTANEOUS EMISSION SIGNALS AT HIGH NITROGEN PARTIAL PRESSURES

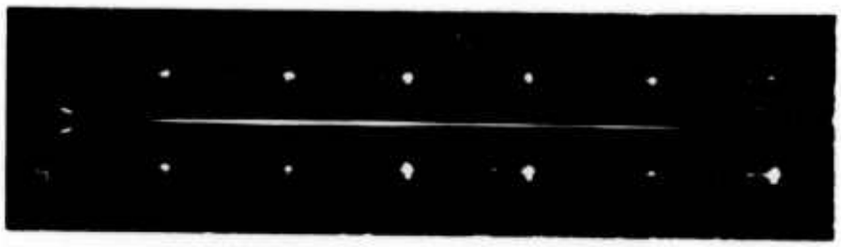

a. PHOTOGRAPH OF DISCHARGE $p = 3.3$ atm, $I_o \approx 8.0 \times 10^8$ W/cm^2

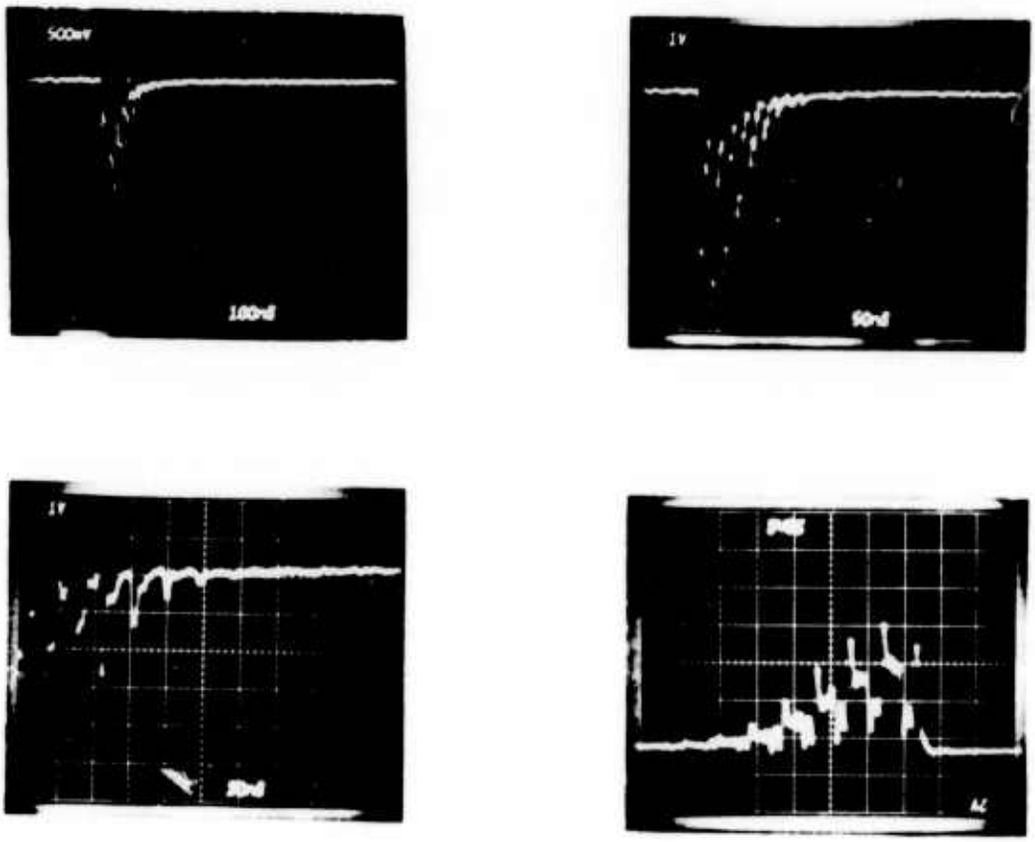

b. PHOTODETECTOR SIGNALS $X_{N_2} = 0.17$, $X_{He} = 0.83$

3371 Å SPONTANEOUS EMISSION SIGNAL AT LOW NITROGEN PARTIAL PRESSURE

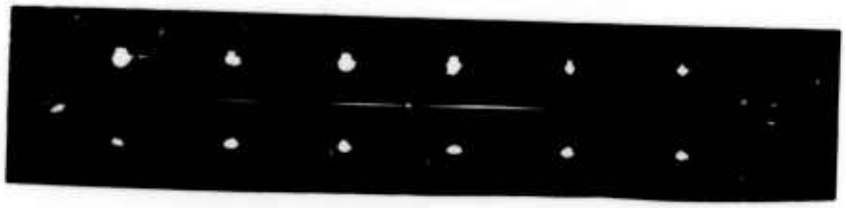

a. PHOTO OF DISCHARGE $p \simeq 2.0$ atm, $I_o \simeq 8 \times 10^7$ W/cm^2

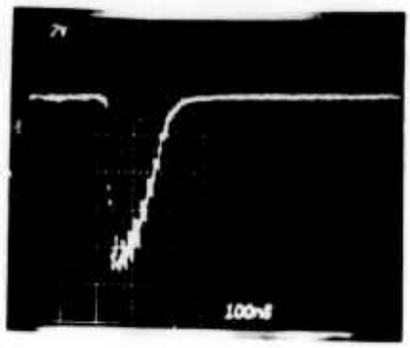

b). SPONTANEOUS EMISSION SIGNAL $X_{N_2} = 0.01$, $X_{He} = 0.99$

3371 Å SPONTANEOUS EMISSION SIGNALS IN $He/Ar/N_2$ MIXTURES

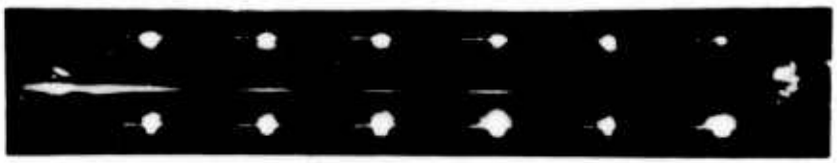

a. PHOTO OF DISCHARGE $p \approx 2.0$ atm, $I_o \approx 1 \times 10^8$ W/cm^2

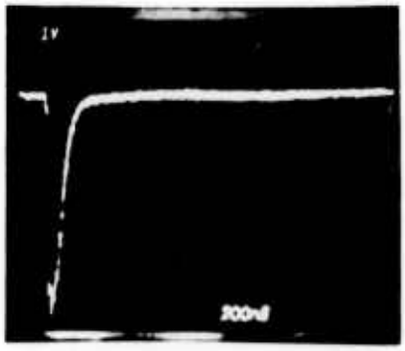

a. $X_{N_2} \approx 0.07$

$X_{Ar} \approx 0.12$, $X_{He} \approx 0.81$

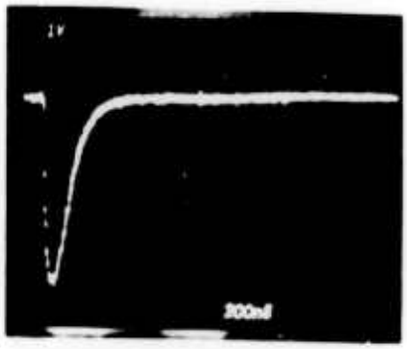

b. $X_{N_2} \approx 0.014$

$X_{Ar} \approx 0.14$, $X_{He} \approx 0.85$

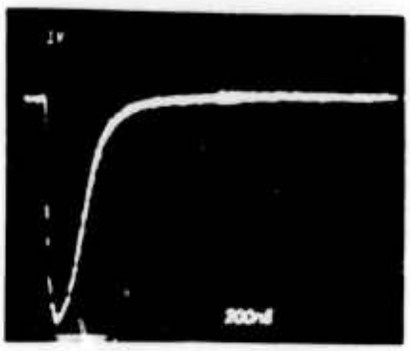

c. $X_{N_2} \approx 0.010$

$X_{Ar} \approx 0.14$, $X_{He} \approx 0.85$

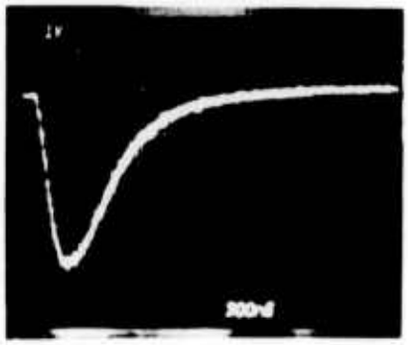

d. $X_{N_2} \approx 0.006$

$X_{Ar} \approx 0.14$, $X_{He} \approx 0.85$

N09-238-8

5.5 Laser Studies

As mentioned in Section 5.3, the transverse pumping approach was not successful, and no attempts were made to operate the transverse cell as a uv laser. In an attempt to obtain uv lasing in cell #1, the arrangement shown in Fig. V-9 was used. A small hole was placed in the 10.6μ focusing mirror, to allow a uv cavity to be placed around the discharge as shown. In operating with this arrangement, three problems were encountered. (1) Small changes in the alignment of the 10.6μ optical train caused the optically pumped discharge to move around in the cell, making it difficult to keep the discharge colinear with the axis of the uv cavity. (2) The length of the uv cavity and the large number of intra-cavity elements made alignment of the uv cavity difficult. (3) At the time these tests were run, a narrow band filter at 3577 Å (the wavelength for strongest lasing, reported in Ref. 3) was not on hand.

Typical photodetector traces obtained with this arrangement are shown in Fig. V-10. It can be seen that there is no apparent change in the 3371Å signal with the cavity in place, indicating that for these conditions lasing did not occur. Within the limits of the experimental setup, conditions were varied in an attempt to achieve lasing , but no signals which could be identified as a clear-cut proof of lasing were obtained.

It is felt that the primary cause of the inability to observe lasing was the rather poor uv optical cavity, rather than any inherent problem in the medium itself. In order to check the operation of the uv cavity (with the various intracavity elements in place), a small, transverse, low-pressure N_2 discharge channel has been fabricated and will be substituted for the OPEDL cell. This channel, which will be operated during the next reporting period, will allow checks to be made on the operation of the uv cavity and the detector system. Also, the OPEDL cell will be operated with a new optical configuration, as described in the next section.

FIG. V-9

uv CAVITY ARRANGEMENT

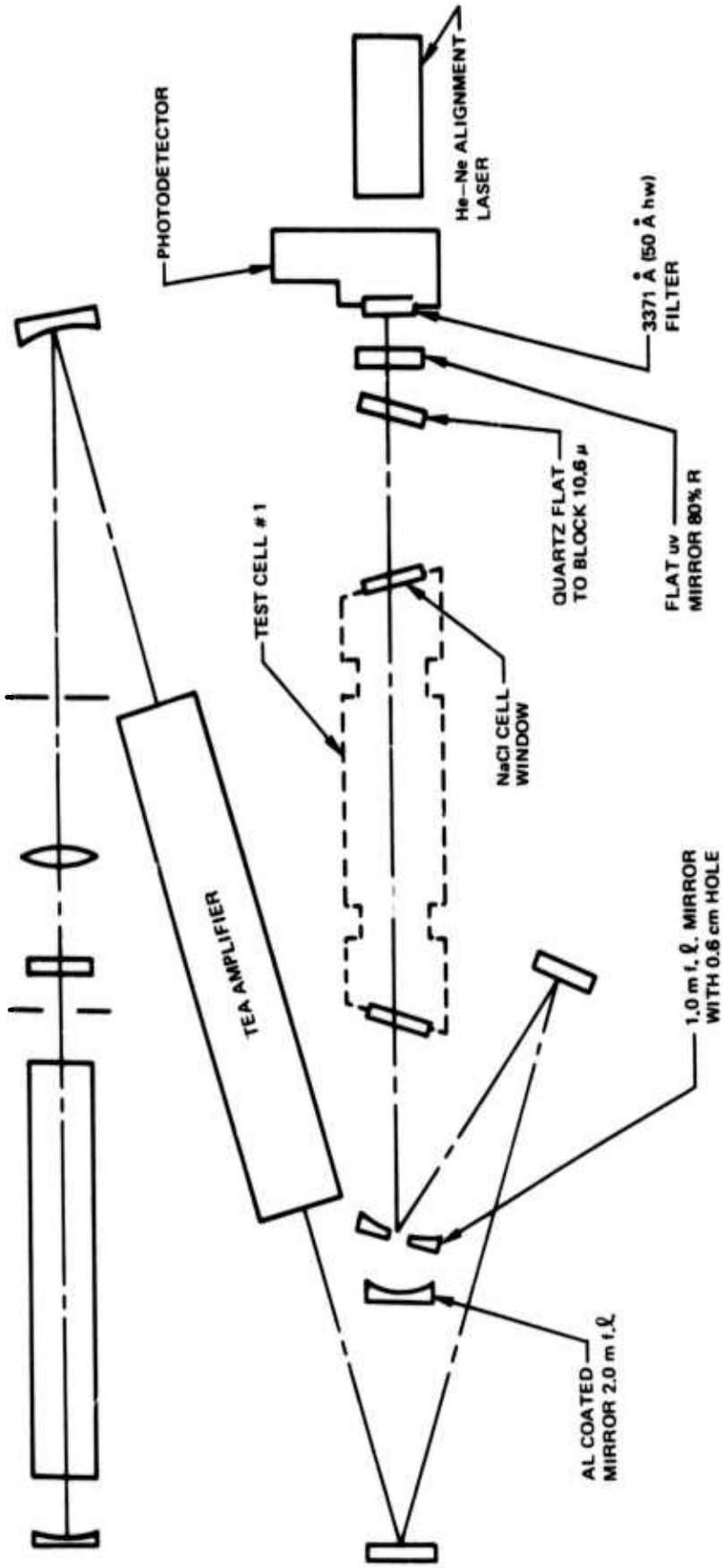

N09-238-18

PHOTODETECTOR TRACES WITH uv CAVITY

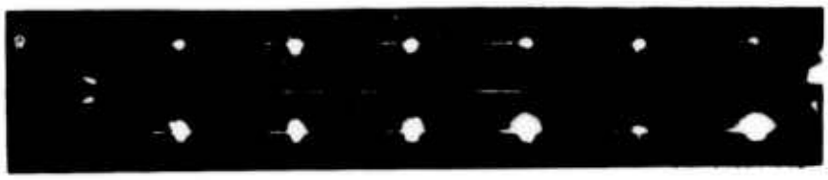

a. PHOTO OF DISCHARGE $p = 2.3$ atm, $I_0 \approx 2.0 \times 10^8$ W/cm^2

$X_{N_2} \approx 0.08$, $X_{Ar} \approx 0.14$, $X_{He} \approx 0.78$

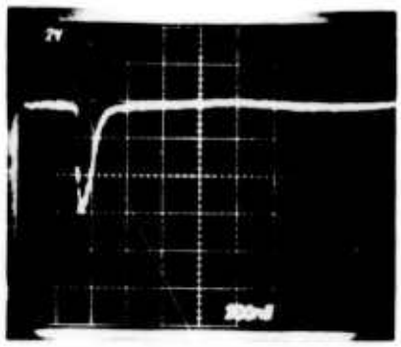

a. NO uv CAVITY

b. WITH uv CAVITY

c. 80% uv MIRROR ONLY

N09 238 15

SECTION VI

PUMPING CONFIGURATION STUDIES

6.1 Introduction

There are various optical configurations which might be considered for the OPEDL. These include the use of annular 10.6μ beams, the use of prisms and gratings to separate the 10.6μ and uv radiation, and the use of 10.6μ cavity-type configurations for pumping. The approach being taken in the present study is to develop a simple configuration which is well suited to the existing experimental setup, and to use this configuration to demonstrate the basic laser properties of the optically-pumped discharge. Once this has been accomplished, studies of various optical configurations, particularly with regard to scaling, would be in order.

6.2 Description of Configuration

An optical configuration which appears to have promise is shown schematically in Fig. VI-1. The 10.6μ beam is reflected off of a conical mirror, forming an annular-cone-shaped beam. This beam is then focused into the cell, forming a focal volume as shown in the figure. This configuration is attractive because it allows the uv mirrors to be mounted internal to the cell, close to the optically-pumped discharge, and at locations where there is no 10.6μ radiation.

6.3 Experimental Studies

A preliminary optical configuration similar to that in Fig. VI-1 was set up using a 2° cone mirror, and a 10.0 cm NaCl lens. Burn patterns at various distances Z (see Fig. VI-1) are shown in Fig. VI-2. For the burn patterns at Z = 8 cm through Z = 28 cm, the 10.6μ beam was attenuated by a factor of 20. From this figure, it can be seen that the region from Z = 16 cm to Z = 24 cm comprizes a region of quasi-uniform intensity in the focal region. This is to be compared with a focal volume length of ~0.01 cm for a colimated gaussian beam and for the 10.0 cm focal-length lens used here. A photograph of gas breakdown spots in laboratory air, obtained with this setup, are shown in Fig. VI-3. This photo is a multiple exposure of 5 TEA laser shots, and based on breakdown data for a 0.5 mm focal diameter[15], shows that the 10.6μ intensity was in excess of 4×10^{8} W/cm^{2} over the length indicated by the breakdown spots. This intensity level is in excess of that required for optical pumping at high pressures.

FIG. VI–1

ANNULAR–CONE PUMPING CONFIGURATION

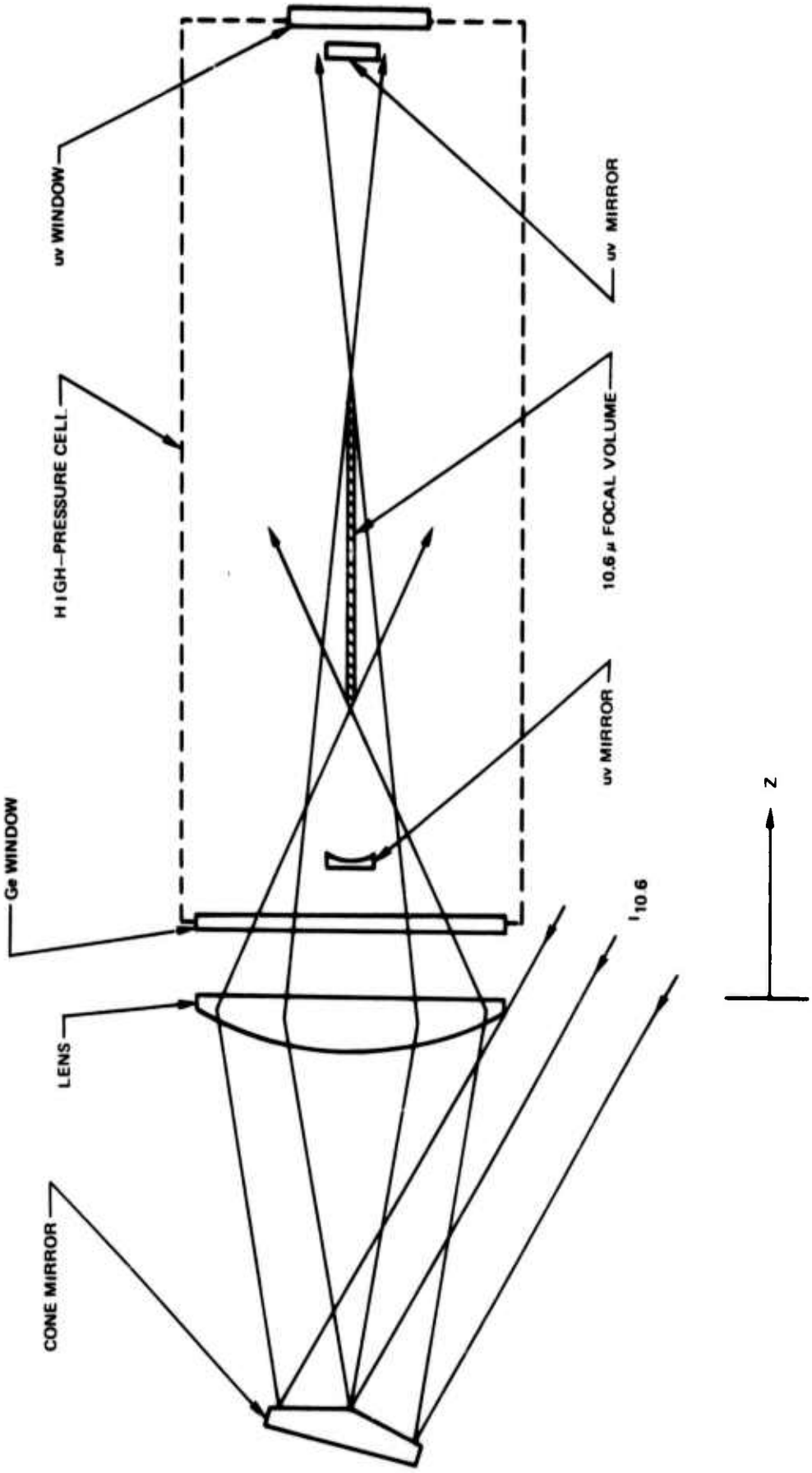

N09–238–21

BEAM PROFILES AT VARIOUS LOCATIONS

BEAM AT CONE

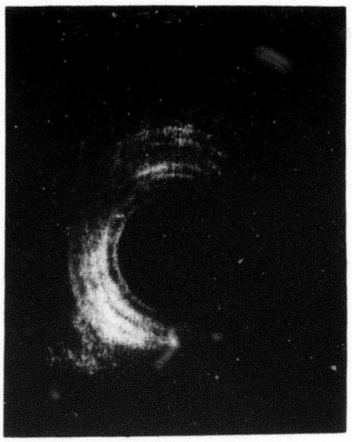

BEAM AT LENS

Z = 2 cm

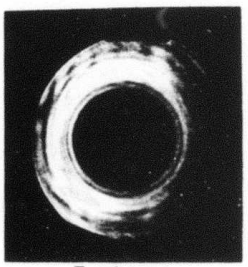

Z = 4 cm

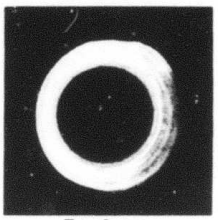

Z = 6 cm

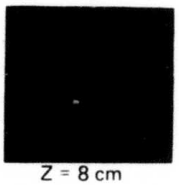

Z = 8 cm

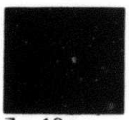

Z = 10 cm

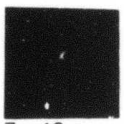

Z = 12 cm

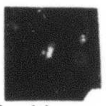

Z = 14 cm

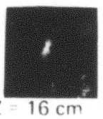

Z = 16 cm

Z = 20 cm

Z = 24 cm

Z = 28 cm

Z = 35 cm

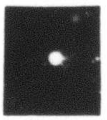

Z = 45 cm

Z = 55 cm

N09 238 24

GAS BREAKDOWN IN LAB AIR WITH ANNULAR–CONE BEAM

$r_1 \ell_1 = 10.0$ cm

This configuration is being studied theoretically, using the complete field equations and including diffraction effects. Preliminary results are shown in Figs. VI-4 and VI-5 for an angle on the reflecting cone of 1° and a lens focal length F of 20.5 cm. These plots are for a gaussian beam with a radius of 1.0 cm. For comparison, the axial intensity corresponding to focusing with a conventional lens which gives the same peak intenstiy at the focus, is shown in Fig. VI-4. These results indicate that the annular-cone configuration should produce a quasi-uniform optically-pumped discharge and will allow the incorporation of uv optics in a straightforward manner.

AXIAL INTENSITY DISTRIBUTION

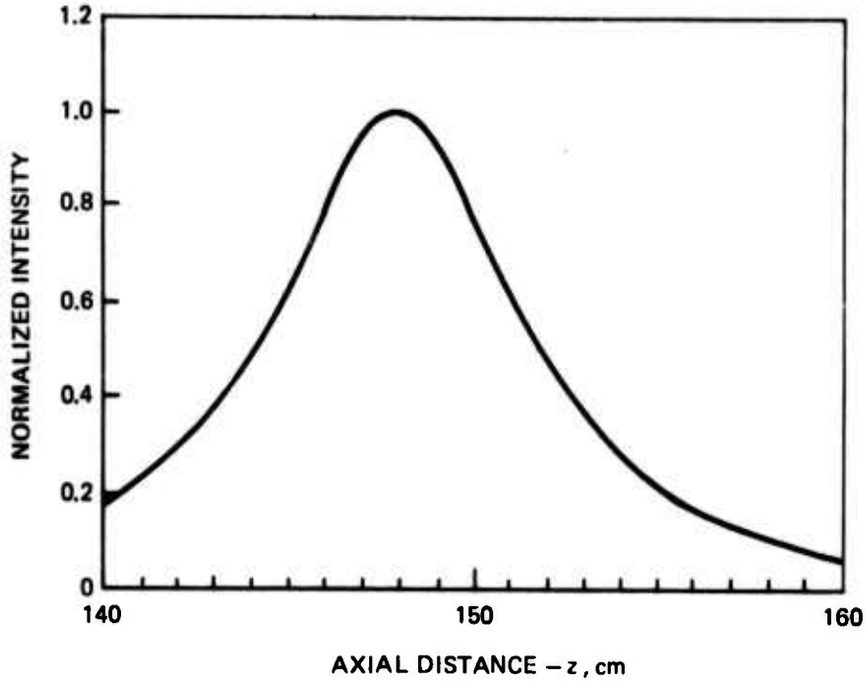

a. $\alpha = 0$, F = 148 cm

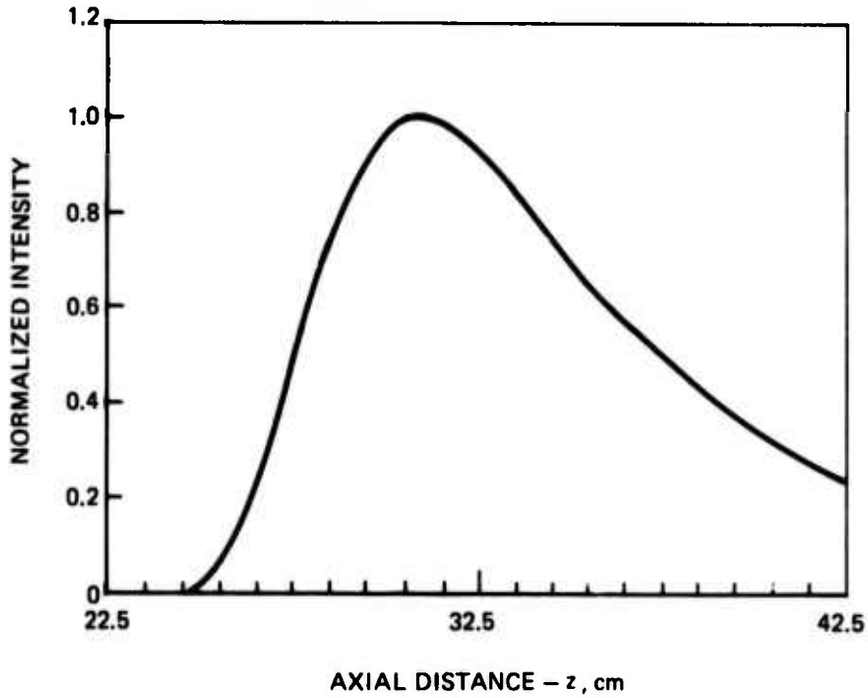

b. $\alpha = 1^{o}$, F = 20.5 cm

TRANSVERSE INTENSITY DISTRIBUTION

$\alpha = 1^{\circ}$, F = 20.5 cm

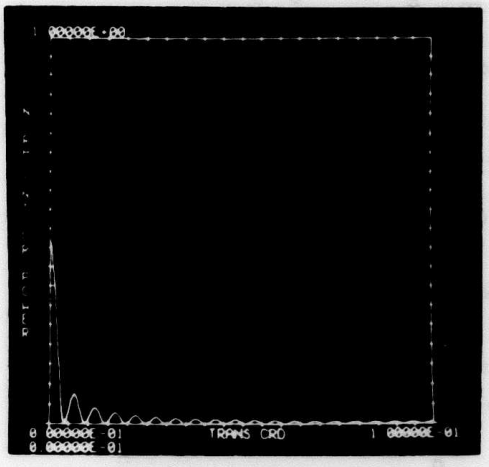

a. Z = 27.5 cm

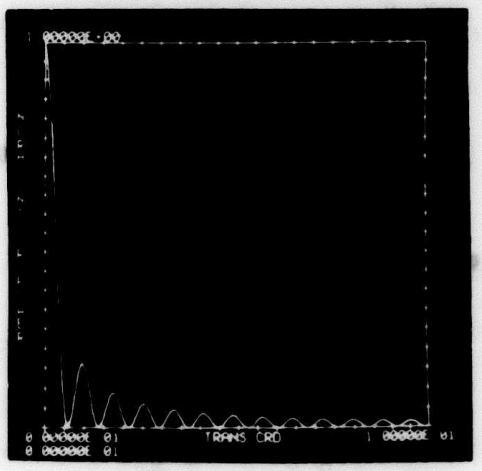

b. Z = 31.0 cm

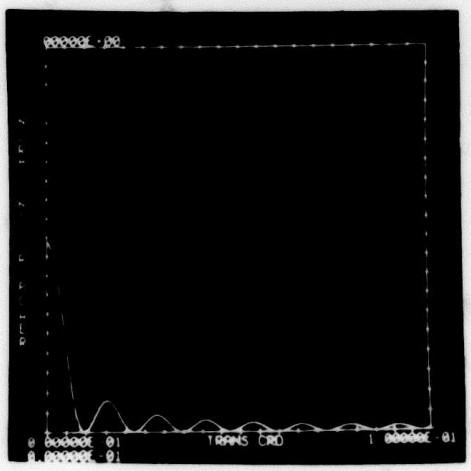

c. Z = 37.5 cm

0 0.1 cm

N09-238-4

SECTION VII

SUMMARY & CONCLUSIONS

The results obtained during the FY'74 program are very encouraging. Diffuse discharges in mixtures of He/N_2 and $He/N_2/Ar$ at electron densities in excess of 10^{15} cm^{-3} and pressures of 15 atm were obtained. These results represent the first time that high-electron-density, high-pressure discharges have been obtained by a technique other than use of a high-energy electron beam. Measurements of the 3371Å spontaneous emission in $He/Ar/N_2$ show that the discharge couples to the excimer level of Ar, which in turn couples to the $C^3\pi$ state of N_2. While theoretical results for $He/N_2/Ar$ have not yet been obtained, results for He/Xe (which is kinetically similar to $He/Ar/N_2$) were obtained and illustrate the high potential efficiency of the OPEDL approach.

Attempts to operate in configurations with a uv optical cavity were not successful; however, this appeared to be due to the lack of an appropriate pumping configuration rather than any fundamental problem in the pumping kinetics. In the near future, studies with a uv cavity will be continued. A small transverse discharge will be used to simulate the optically-pumped discharge in order to check the uv cavity and the detector system. Also, various pumping configurations, including the annular-cone configuration, will be used. Theoretical studies will be continued, and detailed calculations for the $He/Ar/N_2$ system will be carried out.

REFERENCES

1. Shipman, J. D. Jr.: Appl. Phys. Letters 10, p. 3 (1967).

2. Koehler, H. A., L. J. Ferderber, D. L. Redhead, and P. J. Ebert: Appl. Phys. Letters 21, p. 198 (1972).

3. Searles, S. K. And G. A. Hart: Appl. Phys. Letters 25, p. 79 (1974).

4. Collins, C. B., A. J. Cunningham, and M. Stockton: Appl. Phys. Letters 25, p. 344 (1974).

5. Brown, R. T., and D. C. Smith: Appl. Phys. Letters 23, p. 245 (1973).

6. George, E. V. and C. K. Rhodes: Appl. Phys. Letters 23, p. 139 (1973).

7. Lorents, D. C., D. J. Eckstrom, and D. Huestis: Stanford Research Institute Report No. MP 73-2, Sept. 28, 1973.

8. Peterson, L. R., and J. E. Allen, Jr.: J. Chem. Phys. 56, p. 6068 (1972).

9. Gryzinski, M: Phys. Rev. 115, p. 374 (1959).

10. Sheldon, J. W. and J. V. Dugan, Jr., NASA Communication, Lewis Research Center, Cleveland, Ohio, April 17, 1964.

11. Gerardo, J. B., and A. W. Johnson: IEEE J. Quantum Electron. QE-9, p. 748 (1973).

12. Brown, R. T., and D. C. Smith: Appl. Phys. Letters 24, p. 236 (1974) (Appendix I).

13. Beaulieu, J. A.: Proc. IEEE 59, p. 667 (1971).

14. Pan, Yu-Li, A. A. Bernhardt, and J. R. Simpson: Rev. Sci. Instr. 43, p. 662 (1972).

15. Smith, D. C., P. J. Berger, R. T. Brown, and M. C. Fowler: UARL Rept. L921104-6, Final Report on AFWL Contract No. F29601-71-C-0037, Sept. (1972).

16. Eckstrom, D. J., R. A. Gutcheck, R. M. Hill, D. Huestis, and D. C. Lorents,: Stanford Research Institute Report No. MP 73-1, July 31, 1973.

APPENDIX

PUBLICATION REPRINT

Optically pumped electric-discharge uv laser

Robert T. Brown and David C. Smith
United Aircraft Research Laboratories, East Hartford, Connecticut 06108
(Received 6 December 1973)

A new technique for pumping uv laser transitions is described. The technique consists of using an intense 10.6-μ laser pulse to drive a diffuse discharge in a preionized uv laser medium. Because of its fast rise time, high electron density, and ability to operate at high pressure, this discharge is well suited to pumping uv laser transitions. Experimental results are shown for the application of this technique to the 3371-Å transition in nitrogen. A diffuse discharge at atmospheric pressure was obtained, and an intense pulse of 3371-Å radiation was observed.

There is presently a great deal of interest in generating high-energy laser pulses in the uv portion of the spectrum. Previous studies have centered around two techniques for generating such pulses. Low-inductance circuits have been used to produce fast-rising high-current discharges at moderate pressure in order to pump transitions such as the 3371-Å laser transition in molecular nitrogen.[1] More recently, high-energy short-pulse electron beams have been used to produce a high-pressure xenon laser at 1730 Å.[2] The present study describes a technique for using a high-energy 10.6-μ pulse from a TEA laser to drive a diffuse discharge in a high-pressure gas. The properties of this discharge are such that it can be used as the active medium for a uv laser.

The basic elements of this concept can be explained in terms of the arrangement used in the present experiments, as shown in Fig. 1. The output laser pulse from the TEA laser is focused into the active uv laser medium which has been preionized to some low level of electron density (in the present study the preionization was produced via photoionization from two rows of small arcs in the uv laser medium). The 10.6-μ optical field then heats the electrons via inverse bremsstrahlung, and the electron density grows in a cascade process.[3] The size of the discharge produced is determined by the size of the 10.6-μ laser focal volume. Since this discharge can have a very fast rise time (< 10 nsec) and can reach very high electron densities (full ionization, i.e., gas breakdown, for sufficiently high 10.6-μ

 Copyright © 1974 American Institute of Physics

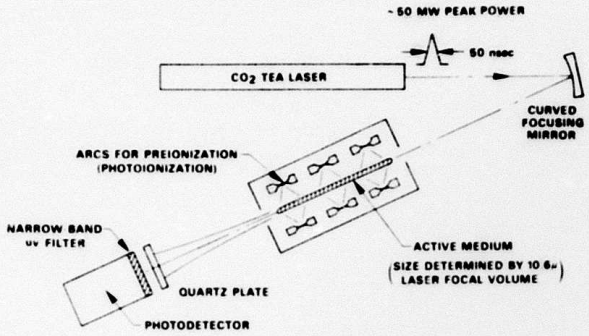

FIG. 1. Diagram of optically pumped electric-discharge laser experiment.

laser fluxes), the discharge should be suitable for pumping various uv laser transitions.

The inverse bremsstrahlung heating process is analogous to rf heating at lower frequencies[4] and can be written in terms of the expression

$$\dot{Q} = n_e e^2 I \nu / m_e \epsilon_0 c(\omega^2 + \nu^2), \qquad (1)$$

where $\dot{Q}$ is the heating rate per unit volume, n_e is the electron density, e is the electronic charge, I is the 10.6-μ laser intensity, ν is the electron-heavy-particle momentum transfer collision frequency, m_e is the electron mass, ϵ_0 is the free-space permittivity, c is the speed of light, and ω is the laser radiation angular frequency. Since the collision frequency ν is proportional to the gas pressure, it can be seen from Eq. (1) that for a given pumping laser wavelength, there is an optimum pressure for maximizing the energy deposition rate to the electrons. For 10.6-μ pumping radiation, and for pure xenon gas, this optimum occurs at approximately 17 atm; and, thus the CO_2 TEA laser (which is the most efficient of the various high-energy short-pulse lasers) is well suited to pumping high-pressure excimer laser media such as xenon.

In the present experiments, the optically pumped electric-discharge laser concept, described above, was applied to the 3371-Å transition in molecular nitrogen. This medium was chosen because of its ability to operate at atmospheric pressure (in the presence of a helium buffer gas) and because of its high optical gain. As indicated in Fig. 1, a quartz plate was used to block the 10.6-μ radiation and to pass the uv radiation to the detector. The uv laser medium was operated with no external optical cavity in an attempt to detect gain via amplified spontaneous emission.

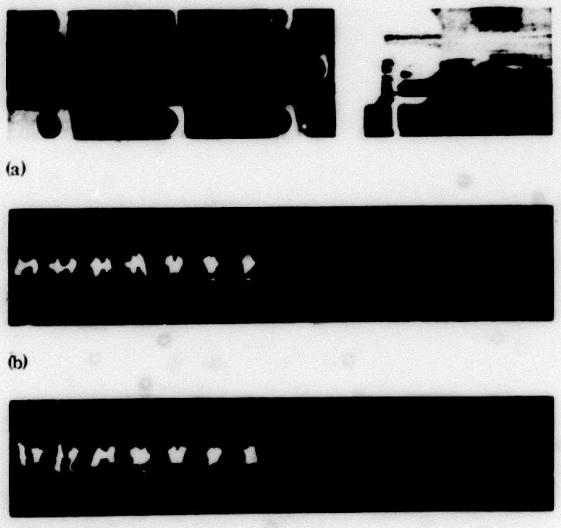

(a)

(b)

(c)

FIG. 2. Photographs of optically pumped discharge (95% He, 5% N_2 at 1.0 atm). (a) Discharge channel assembly. (b) Preionization arcs only. (c) Preionization arcs plus 10.6-μ laser pulse (~5.0 μsec delay).

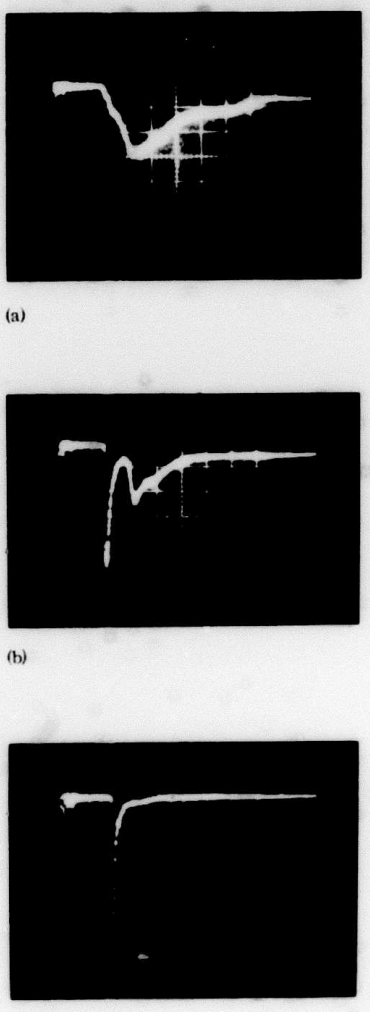

(a)

(b)

(c)

FIG. 3. uv detector signal ($U_0 \approx 1.6 \times 10^9$ W/cm^2, He + N_2 at 1.0 atm). (a) No N_2. Large breakdown observed at end of channel toward laser. (b) 0.2% N_2. Breakdown observed at end of channel toward laser. (c) 4.6% N_2. No breakdown observed. Scale: 500 nsec/div.

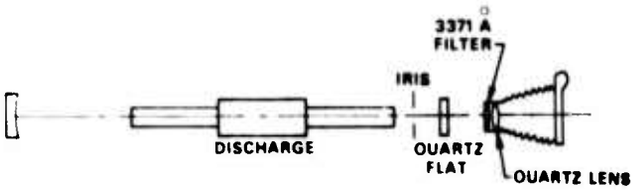

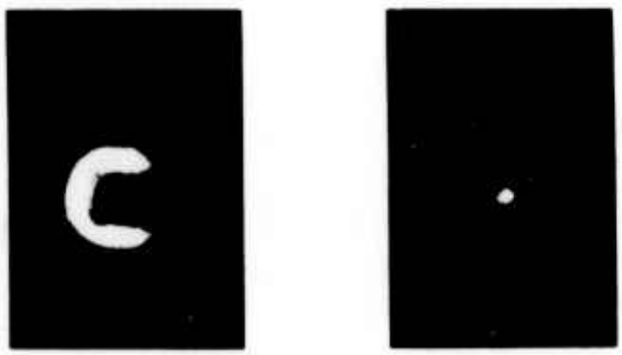

(a) (b)

FIG. 4. Photograph of optically pumped 3371-Å radiation. (a) Photo of discharge channel with background lighting (no 3371-Å filter). (b) Photo of uv radiation spot (single shot, with 3371-Å filter, no breakdown).

Figure 2 shows a photograph of the optically pumped discharge, with the 10.6-μ beam passing between two rows of small arcs in a mixture of 95% He, 5% N_2 at atmospheric pressure. The peak 10.6-μ power in this case was ~50 MW and was focused with a 2.0-m-focal-length mirror, giving a peak intensity I_0 of 2.8×10^9 W/cm^2, and a focal volume 1.5 mm in diameter by 30 cm long. In Fig. 2(c), the optically pumped discharged can be seen extending into the Pyrex tube on the right-hand side of the channel and indicates that the uv preionization was effective over a distance of at least 15 cm. This photograph clearly shows that optical pumping is capable of generating a diffuse discharge at high pressure.

The uv detector used in the present experiments was a phototube with a narrow-band filter (50-Å half-width) centered at 3371 Å, and was situated as shown in Fig. 1. Detector output traces for a range of nitrogen concentrations are shown in Fig. 3. In Fig. 3(a), the discharge was driven to full ionization, and the signal represents the continuum radiation from the helium breakdown plasma. As the nitrogen fraction was increased, maintaining the 10.6-μ laser energy constant from shot to shot, two major effects were observed: (i) An intense spike of radiation at 3371 Å was observed to occur during the rising portion of the 10.6-μ pulse. By using various neutral density filters, it was determined that the peak intensity of the signal increased approximately exponentially with 10.6-μ intensity, and that for conditions of strong pumping, the 3371-Å signal had a half-width of ~20 nsec. Because of the relatively short length of the active discharge (~15 cm at high N_2 fractions), the transition was far below saturation and the total amount of uv energy at the detector was very small ($< 10^{-6}$ J). (ii) As the nitrogen fraction was increased the additional electron energy losses reduced the level of ionization reached during the TEA laser pulse. For conditions corresponding to Fig. 3(c), no breakdown occurred, and only a diffuse discharge extending throughout the focal volume [as in Fig. 2(c)] was observed. The phototube signal for this case was then due strictly to 3371-Å radiation emitted along the diffuse discharge.

Figure 4 shows a photograph of the uv radiation emitted by the discharge. The field of view is shown in Fig. 4(a), and the imaged 3371-Å emission is shown in Fig. 4(b). This photo, taken under conditions of no breakdown, shows a well-defined region of intense uv radiation.

While the above results do not constitute a proof of lasing as such,[5] they do in fact demonstrate the possibility of producing a uv laser with an optically pumped electric discharge. The kinetics of the second positive nitrogen system are well understood,[6] and it is known that if a fast-rising diffuse discharge of sufficient length can be obtained in a helium-nitrogen mixture, lasing via amplified spontaneous emission results.[7] In addition, the above results demonstrate the possibility of obtaining an intense diffuse discharge at high pressure, with a rise time fast enough to pump short-lifetime transitions (e.g., 40 nsec in the case of the 3371-Å nitrogen transition).

The present experiments are being continued in an effort to increase the 3371-Å energy from the uv discharge by (i) increasing the 10.6-μ pumping energy, allowing the use of a larger focal volume, (ii) operating at higher pressures, where the energy input to the electrons is more effective, and (iii) operating with pumping configurations which allow the use of an optical cavity.

In summary, the present experiments have demonstrated a new technique for pumping uv laser transitions. This technique offers significant advantages in rise time, simplicity, efficiency, and scalability over techniques presently being used.

The authors wish to express their thanks to L.J. Muldrew for his assistance in carrying out the experiments.

[1]J.D. Shipman, Jr., Appl. Phys. Lett. 10, 3 (1967).
[2]H.A. Koehler, L.J. Ferderber, D.L. Redhead, and P.J. Ebert, Appl. Phys. Lett. 21, 198 (1972).
[3]R.T. Brown and D.C. Smith, Appl. Phys. Lett. 22, 245 (1973).
[4]Yu. P. Raizer, Sov. Phys.-Usp. 8, 650 (1966).
[5]R.W. Waynant, Laser Focus 9, 41 (1973).
[6]E.T. Gerry, Appl. Phys. Lett. 7, 4 (1965).
[7]Preliminary experiments by the authors with a conventional transverse nitrogen laser showed that in a mixture of 14% N_2, 86% He at atmospheric pressure, lasing could be obtained for lengths as short as 20 cm.

55